Tectonophysics 484 (2010) 4–26

Contents lists available at ScienceDirect

Tectonophysics

journal homepage: www.elsevier.com/locate/tecto

The equivalent elastic thickness (T_e), seismicity and the long-term rheology of continental lithosphere: Time to burn-out "crème brûlée"? Insights from large-scale geodynamic modeling

E.B. Burov

ISTEP - UMR CNRS 7193, University of Pierre and Marie Curie (UPMC), 4 Place Jussieu, 75252 Paris Cedex 05, France

ARTICLE INFO

Article history:
Received 16 February 2009
Received in revised form 7 May 2009
Accepted 10 June 2009
Available online 21 June 2009

Keywords:
Equivalent elastic thickness
Continental rheology
Seismogenic layer
Numerical modeling
Mechanics of the lithosphere

ABSTRACT

Depending on the conditions and time scale, the lithosphere exhibits elastic, brittle-plastic or viscous-ductile properties. As suggested by rock mechanics experiments, a large part of the long-term lithospheric strength is supported in the ductile regime. Unfortunately, these data, validated for strain rates $\sim 10^{-6}\,s^{-1}$, small scales (few cm) and simplified conditions, cannot be univocally interpolated to geological time and spatial scales (strain rates $\sim 10^{-17}$–$10^{-13}\,s^{-1}$, 100–1000 km spatial scales, complex conditions) without additional parameterization. An adequate parameterization has to be based on "real-time" observations of large-scale deformation. Indeed, for the oceanic lithosphere, the Goetze and Evan's brittle-elastic-ductile yield strength envelopes derived from data of experimental rock mechanics were successfully validated by a number of geodynamic scale observations such as the observations of plate flexure and the associated T_e (equivalent elastic thickness) estimates. Yet, for continents, the uncertainties of flexural models and of the other data sources are much stronger due to the complex structure and history of continental plates. For example, in one continental rheology model, dubbed "jelly sandwich", the strength mainly resides in the crust and mantle, while in another, dubbed "crème-brûlée", the mantle is weak and the strength is limited to the upper crust. These models have arisen because of conflicting results from distributed earthquake, elastic thickness (T_e) and rheology data. We address these problems by examining the plausibility of each rheological model from general physical considerations. We review the elastic thickness (T_e) estimates and their relationship to the seismogenic layer thickness (T_s) to show that these two quantities have no direct physical relation. We also show that some of small T_e must be artifacts of inconsistent formulation of the mechanical problem in some Free-Air anomaly admittance models. We point out that this does not necessarily detract from the admittance method itself but refers to its incorrect application in the continental domain. We then explore, by analytical and numerical thermo-mechanical modeling, the implications of a weak and strong mantle for tectonic structural styles. We conclude that rheological models such as crème-brûlée, which invoke a weak lithosphere mantle, are generally incompatible with observations. The jelly sandwich is in better agreement and we believe provides a useful first-order explanation for the long-term support of the Earth's main surface features.

1. Introduction

Recent discussions on the possible relationships between distributed seismicity and long-term rheology of the lithosphere (Maggi et al., 2000; Jackson, 2002; Watts and Burov, 2003; Handy and Brun, 2004; Burov and Watts, 2006) have revealed a number of problems concerning the assessment of short- and long-term mechanical properties of the lithosphere. These discussions were partly fuelled by: (1) the attractiveness of the possibility to relate real-time, human scale observations to long-term rheological behaviour; (2) some reports on "correlation" between T_s (the seismogenic layer thickness) and T_e (the equivalent elastic thickness of the lithosphere).

The strength of the lithosphere has been a topic of debate ever since the turn of the last century since the introduction of this term by Barrell (1914) who has defined it as a strong outer layer that overlies a weak fluid asthenosphere. This concept played a major role in the development of plate tectonics (e.g. Le Pichon et al., 1973) and the question of how the strength of the plates varies spatially and temporally is a fundamental one of wide interest in geology and geodynamics.

The primary proxy for strength of the lithosphere is the equivalent elastic thickness, T_e (see Watts, 2001 and references therein). By comparing observations of flexure in the region of long-term loads such as ice, sediment and volcanoes to the predictions of simple elastic plate (flexure) models, it has been possible to estimate T_e in a wide

Fax: +33144275085.
E-mail address: evgenii.burov@upmc.fr.

0040-1951/$ – see front matter © 2009 Elsevier B.V. All rights reserved.
doi:10.1016/j.tecto.2009.06.013

range of geological settings. Oceanic flexure studies suggest that T_e is in the range 2–40 km and depends on load and plate age. In the continents, however, T_e ranges from 0 to 100 km and shows no clear relationship with age.

The results of flexure studies are qualitatively consistent with the results of experimental rock mechanics. The Brace–Goetze failure envelope curves (Goetze and Evans, 1979; Brace and Kohlstedt, 1980), for example, predict that strength increases with depth and then decreases in accordance with the brittle (e.g. Byerlee, 1978) and ductile deformation laws. In oceanic regions, the envelopes are approximately symmetric about the depth of the brittle–ductile transition (BDT) where the brittle-elastic and elastic-ductile layers contribute equally to the strength. Since both T_e and the BDT generally exceed the mean thickness of the oceanic crust (~7 km) then the largest contribution to the strength of oceanic lithosphere must come from the mantle, not the crust. In the continents, the envelopes are more complex and there maybe more than one brittle and ductile layer. Despite this, Burov and Diament (1995) have been able to show that a model in which a weak lower crust is "sandwiched" between a strong brittle-elastic upper crust and an elastic-ductile mantle accounts for the wide range of T_e values observed due to the wide variation in composition, geothermal gradient, and crustal thickness possible in continental lithosphere. We regard as "jelly-sandwich" (hereafter JS) all rheology models that include strong mantle layer and a weak layer somewhere in the crust, not necessary in the lower crust (e.g., Fig. 1a, bottom case c). For cratons, there is a possibility that the entire crust and mantle are strong (Burov and Diament, 1995).

Recently, Jackson (2002) challenged the JS model for the rheology of continental lithosphere. Following McKenzie and Fairhead (1997), he stated the model was incorrect, proposing instead a model in which the crust is strong, but the mantle is weak. We dubbed this the "crème-brûlée" model (hereafter CB, Watts and Burov, 2003; Burov and Watts, 2006, Fig. 1a). Jackson (2002) bases his model on the observations of Maggi et al. (2000) which suggest that earthquakes in the continents are restricted to a single layer (identified as the seismogenic thickness, T_s) in the uppermost brittle part of the crust, and are either rare or absent in the underlying mantle.

Still, there is no strong mechanical argument in favour of the idea that seismic sliding may have a direct link to the long-term deformation. Seismic deformation occurs at strain rates that exceed the geological strain rates by a huge factor of 10^{20}. Dislocation or diffusion creep in the lithosphere cannot be physically activated at such strain rates, and thus, in its response to seismic solicitation, the bulk of the lithosphere must react as an elastic/elastic–plastic body. For the mantle lithosphere this is rather incontestable since in there, seismic shear waves have nearly same attenuation as an ideal elastic medium. The only explanation to the possible links between seismic and long-term rheology refers to the hypothesis that the distributed earthquakes take place in a "historically" pre-fractured layer, which thickness is controlled by the depth to the long-term brittle ductile transition (BDT). It is also suggested (Maggi, personal communication) that the earthquakes should happen in a historically "stiff" layer, which can "accumulate" elastic stress released during earthquakes. Yet, this argument does not hold for geological time-scale processes since the inter-seismic cycles occur at periods of time (<1–100 yr) that are 10–1000 times shorter than the crustal relaxation times predicted from CB rheology. Consequently, the only testable idea refers to that of the historically pre-fractured brittle layer limited by the long-term BDT zone. The depth of the BDT zone depends on temperature and strain-rate distribution and brittle and ductile properties of the rocks.

The experimental rock mechanics data are based on relatively low temperatures and pressures, and strain rates that are orders of magnitude greater than those that apply to the lithosphere (~at best $10^{-10}\,s^{-1}$, in average 10^{-6}–$10^{-4}\,s^{-1}$ compared to geological ~10^{-17}–$10^{-13}\,s^{-1}$). Hence, it is not easy to use these data to distinguish between different rheological models (e.g. Rutter and Brodie, 1991). Moreover, construction of YSE (Yield Strength Envelopes) from data of rock mechanics requires additional (yet poorly constrained) information such as temperature profile with depth, lithology, fluid content and strain rate distribution. For example, based on the same data as Jackson (2002) one can derive both an YSE with very weak and very strong rheological envelope (Fig. 1b) for the continental lithosphere: Jackson (2002) has assumed that the thermal and lithological structure of the Earth is identical to that of Venus (Mackwell et al., 1998). This assumption of thin lithosphere with hot mantle and relatively cold crust yields characteristic "CB" YSE. Based on Earth data, we are confident, however, that the Earth's continental lithosphere is thicker than the Venusian lithosphere and has a colder mantle temperature gradient. This only difference yields "JS" YSE for the same rheological parameters as those used by Jackson (2002). In this study, we therefore take a different approach. First, we review the T_e estimates because they, we believe, best reflect the integrated strength of the lithosphere. Then, we use numerical models to test the stability and structural styles associated with the various rheological models. In order to focus the debate, we limit our study here to the rheological models considered by Jackson (2002): crème-brûlée and jelly sandwich.

2. Gravity anomalies and T_e

Isostatic gravity anomalies, i.e. departures of the observed gravity signal from the predictions of local isostatic models (e.g. Airy, Pratt), have long played a key role in the debate concerning the strength of the lithosphere. These data are usually presented in pre-processed form of Free-Air gravity anomaly or Bouguer gravity anomaly. Both correspond to a difference between the observed absolute gravity signal and the theoretical gravity signal that could have been observed at the measurement point under certain assumptions about the reference model of the Earth. Isostatic anomalies refer to the difference between the observed gravity anomaly (Free-Air or Bouguer) and that predicted by a reference mechanical model (e.g. Airy) of isostatic compensation of the observed surface and subsurface loads.

There is common yet mistaken opinion that Free-Air gravity anomaly (FAA) data are "true" data compared to "pre-processed, over-corrected" Bouguer gravity anomaly. This is incorrect. In the continental domain the observations are performed at certain elevation h above or below the surface of the reference model of the Earth (sea-level, reference ellipsoid or geoid). As very clearly stated first by Naudy and Neumann (1965) and recalled in many studies since (e.g. Ervin, 1977; Patella, 1988; Lafehr, 1991; Chapin, 1996; Li and Götze, 2001; Hackney and Featherstone, 2003; Fairhead et al., 2003), the Free-Air correction consists in computing a theoretical value at the measurement altitude without taking into account the gravitational effect of the material in between ellipsoid (where theoretical formulae is computed) and the surface measurement. The standard correction Free-Air (FA) correction is a simple upward/downward correction based on the idea of spherically homogeneous Earth. The Free-Air gravity anomaly is defined as a difference between the measured signal and Free-Air corrected theoretical gravity. In oceans, measurements are done at sea surface (h~0) so that the corresponding FA correction is zero. But in continents, contrary to some ideas, the continental Free-Air (FAA) gravity anomalies are not "rough" data. The FA correction is roughly equal to ~$0.3086\times h$ (mGal). It is actually the strongest modification (300 mGal per km of elevation) applied to the data. This correction is subject to quite important errors characterized by quite large spectral bandwidths, from long-wavelength harmonics arising from an incompatibility between the geometry of the reference ellipsoid and the assumption of perfect sphericity of the Earth used for derivation of FAA, to very short-wavelengths associated with the absence of terrain corrections, near-surface density anomalies, instrumental and gridding errors.

The Bouguer correction is aimed to correct the theoretical gravity from the effect of excess/default masses that are known and not taken into account by the Free-Air formulae. Namely this is the excess mass of topography on land and the default mass in oceans due to the fact that the oceans consist of water and not rocks. In other terms (for geophysicists) the Bouguer anomaly reflects the mass heterogeneities beneath the surface measurements (assuming in the oceans that the water has been replaced by denser material and therefore there is no more sea bottom topography effect). In continents, the so-called simple Bouguer correction Δ_{bg} is usually equal to $4.19 \times 10^{-5} \rho h$ (mGal), which yields $0.1118 \times h$ (mGal) for commonly inferred effective crustal density (ρ) value of 2670 kg/m^3. Compared to the FAA correction, the Bouguer correction presents a smaller modification of the initial data. The simple Bouguer formula corresponds to the gravity effect of an infinite plateau of thickness h and provides only a first-order approximate correction for the effect of real 3D topography. The gravity measuring instruments (gravimeters) measure only the vertical component of the gravity field. Compared to the assumption of a flat

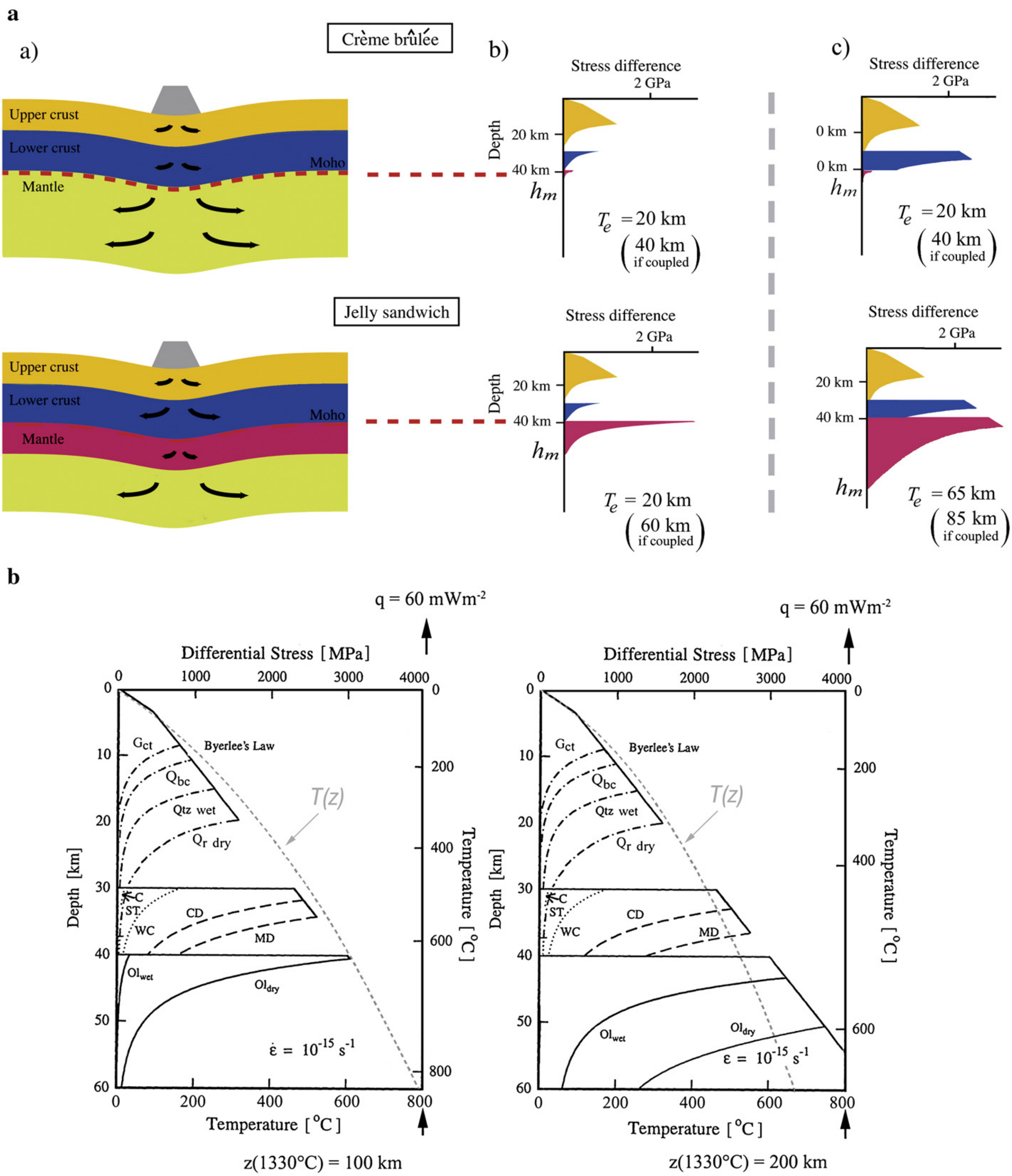

Earth, this component can be reduced or increased due to the lateral attraction from anomalous masses associated with local relief. For that, additional terrain corrections are applied to account for the 3D effect of topography gradients in close vicinity (sometimes first meters) of the data point. These corrections are usually made *in situ*, at same time as measurements, and are of crucial importance in the areas of undulated topography such as mountain ranges. What is usually called Bouguer correction refers to the complete Bouguer correction, which includes both the simple Bouguer correction and terrain correction. The complete Bouguer gravity anomaly is a Free-Air gravity anomaly additionally corrected using simple Bouguer and terrain correction.

Standard flat-Earth FAA is not terrain-corrected, which is a significant drawback limiting its application in continents. Contrary to what is sometimes asserted, it is impossible, or very difficult, to post-correct the existing gridded FAA data, because the information on terrain corrections is usually not preserved and normally cannot be recovered, since such operation would require the exact knowledge of the location of the initial data points and of the surrounding topography, with spatial resolution higher than that of usual digital terrain models.

The spectra of continental FAA anomaly is dominated by short wavelength topographic components, which correlate with the unaccounted terrain effects (the higher is the local topography, the stronger are the would-be terrain corrections because the terrain roughness correlates with the average elevation), short wavelength instrumental and gridding/sampling errors. Consequently, the use of FAA in spectral gravity methods may result in shifts towards shorter frequencies and thus to an overestimation of the influence of local topography on the observed gravity anomaly, which results in underestimated T_e values. In cratonic areas, short-wavelength surface topography has little to do with the large-scale deformation (Burov et al., 1998), and the generally weak gravity signal is highly influenced by unaccounted subsurface heterogeneities of various kinds. This may partly explain the low EET estimates obtained by McKenzie and Fairhead (1997) from FAA-based inverse gravity modelling (the main part of the explanation is provided in the next sections).

The effect of complete Bouguer correction is opposite to that of the FAA correction. It tends to enhance the signal due to the Moho depression by decreasing the contribution from parasite short-wavelength components such as terrain effects, gridding errors and small-scale heterogeneities. One can argue (McKenzie and Fairhead, 1997) that Bouguer correction may generate shifts towards longer wavelengths and thus to over-estimated T_e values. However, the wavelength of low-pass signal smoothing that can be produced by Bouguer correction is on the order of the distance from the surface to the Moho depth (~35 km in average). Plate bending generates wavelengths on the order of 5–10T_e. Consequently, T_e values higher than 10 km would not be affected. On the other hand, flexural deformation associated with T_e values smaller than 10 km is unlikely to be robustly differentiated from simple local compensation ($T_e = 0$ km) as topography wavelengths smaller than 50 km can be well associated with many small-scale deformational mechanisms such as folding and faulting of the sedimentary cover and uppermost basement rock.

Whatever are the advantages and disadvantages of FAA or Bouguer gravity data for flexural modelling, if similarly formulated, both FAA and Bouguer-based models should have provided more similar results (Pérez-Gussinyé and Watts, 2005) than those obtained by Jackson (2002) and McKenzie and Fairhead (1997) from FAA admittance, compared to the models based on Bouguer coherence. We will later show that the major deviations between the FAA and Bouguer based inverse gravity models in continental domain most probably stem from different formulation of the mechanical kernels of these models, and not from the data itself. In particular, the use of FAA-based gravity admittance strongly limits the possibility of adequate formulation of the flexural model in continental domain. Bouguer-based coherence models are more flexible in these terms.

Modern isostatic studies follow either pure forward or inverse modelling approach. The forward approach (e.g., Burov et al., 1990; Burov and Molnar, 1998) allows one to take into account all loads, plate boundaries and forces exerted on the lithosphere. Inverse modelling approaches work with simplified mechanical kernels that do not account for plate boundaries and boundary forces and, in worst case, for surface or subsurface loads. In forward modelling, the gravity anomaly due, for example, to a surface (i.e. topographic) load and its flexural compensation is calculated for different values of T_e and compared with the observed gravity anomaly. The 'best fit' T_e is then determined as the one that minimises the difference between observed and calculated gravity anomalies. The forward models allow to account for versatile boundary conditions and plate boundaries (end forces and moments, subsurface loads etc). In inverse (mainly spectral) models, gravity and topography data are used to estimate T_e *directly* by computing the transfer function between them as a function of wavelength and comparing it to model predictions. The mechanical part of the spectral models is simplified as technically it is very difficult to account for certain normal loads and specifically for plate boundaries and forces in spectral domain. These models basically assume periodic or reflecting boundary conditions, which makes them inapplicable near plate boundaries with important topography or tectonic loading conditions (i.e. Himalaya). While the forward models are more robust and, in particular, insensitive to the choice of the modelled gravity anomaly, Bouguer or FAA, the different approaches should yield same results if their mechanical problem is formulated identically, both in terms of surface and subsurface loads, internal boundary conditions and of the area chosen for modelling. It is rarely the case, since, while the forward models have no particular limitations, the inverse methods are bound to use reflecting or periodic

Fig. 1. a. Schematic diagram illustrating different models for the long-term (>10^6 a) strength of continental lithosphere (after Burov and Watts, 2006). In the crème-brûlée model, the strength is confined to the uppermost brittle layer of the crust and compensation is achieved mainly by flow in the weak upper mantle. In the jelly sandwich model, the mantle is strong and the compensation for surface loads occurs mainly in the underlying asthenosphere. a) Model of deformation. The arrows schematically show the velocity field of the flow. b) Brace–Goetze failure envelopes for a thermo-tectonic age of 150 Myr, a weak undried granulite lower crust, a uniform strain rate of 10^{-15} s^{-1}, and either a dry (jelly sandwich) or wet (crème-brûlée) olivine mantle. Other parameters are given in Table 1. The envelopes, which match those in Figs. 5B and D of Jackson (2002), yield a T_e of 20 km (Burov and Diament, 1995). c) Brace-Goetze failure envelopes for a thermo-tectonic age of 500 Myr. Other parameters are as in b) except that a strong dry Maryland diabase has been used for the lower crust. The envelopes show two other possible rheological models for continental lithosphere: one in which the upper and lower crust are strong and the mantle is weak (upper panel) and another in which the upper and lower crust and the mantle are strong (lower panel). h_m is the mechanical thickness of the lithosphere. In case of mechanical decoupling between the competent layers (i.e. when they are interleaved with weak zones as in case b), T_e is smaller than a sum of layer thicknesses. In this case it is close to the thickness of the largest competent layer or zone (Burov and Diament, 1995). For example, the presence of strong diabase lower crust in the upper case c) or of the mantle in the bottom case b) almost does not add to T_e. In the former case, T_e could rise to maximum of 40 km only if the upper crust was strong at the transition with the lower crust. Yet, the strength of the diabase crust adds to T_e in the bottom case c) since the lower crust is strong at the transition with the mantle lithosphere (i.e. the layers are mechanically coupled). b. Influence of compositional variation, plate thickness $a = z(1330\ °C)$ and fluid content on continental Yield Stress Envelope (YSE) computed for typical surface heat flow, q, of 60 mW m^{-2} but two different thermal models: equilibrium thermal plate thickness of 100 km (left, Chapman, 1986) and of 200 km (right, plate cooling model, Appendix B, (Burov and Diament, 1995). CD — dry Columbia diabase, MD — dry Maryland Diabase, WC — Pikwitonei granulate, ST and C — diabase from (Shelton and Tullis, 1981) and (Caristan, 1982). The upper crust is wet quartzite from Gleason and Tullis (1995), Ol_{dry} and Ol_{wet} — dry and wet dunite from (Chopra and Paterson, 1984). Q_{bc} refers to dry quartzite from Brace and Kohlstedt (1980). G_{gt} is wet granite from Carter and Tsenn (1987). Qr is for extra strong dry quartz from Ranalli (1995). Comparison of the YSE computed for two different thermal plate thicknesses demonstrates large ambiguities in estimation of the mantle strength: the continental heat flux used as a common surface boundary condition mainly affects crustal temperature distribution. The mantle part of the geotherm primarily depends on the position of the thermal bottom of the lithosphere. The left "weak" YSE results from erroneous assumption that continents have the same or even smaller thickness than the oceans (Jackson, 2002). The use of the left YSE results in unrealistically small predictions of the mantle strength. The failure envelope shown on the left match that from Jackson (2002), which is based Fig. 4 from Mackwell et al. (1998) derived for Venus. The parameters are given in Table 1.

boundary conditions that neglect boundary forces and, in worst cases (i.e. FAA admittance) cannot handle surface topography loads. In particular, previous work has shown that the estimates of the admittance between topography and Free-Air gravity anomalies are often biased by spectral leakage (e.g., Crosby, 2007).

In oceanic regions, surface topography coincides with sea level and gravity is also measured at sea level, that is at some vertical distance from the possibly ragged sea floor. Then, a parasite contribution from local sea-bottom topography slopes is naturally attenuated and the treatment of the measured signal does not require terrain correction (nor generally Bouguer correction *sensu stricto* since $\underline{h}=0$). In this case forward flexural models and inverse admittance or coherence methods yield similar T_e values. This is well seen along the Hawaiian–Emperor seamount chain in the Pacific Ocean. Forward modelling reveals a mean T_e of 25 ± 9 km while inverse (spectral) modelling using a Free-Air admittance method obtains 20–30 km (Watts, 1978). When the T_e estimates are plotted as a function of load and plate age they yield the same result (Fig. 5): T_e increases with age of the lithosphere at the time of loading, being small (2–6 km) over young lithosphere and large over old lithosphere (>30 km, Fig. 2b).

In continental regions, the two modelling approaches have yielded different results. The earliest spectral studies, for example, recovered

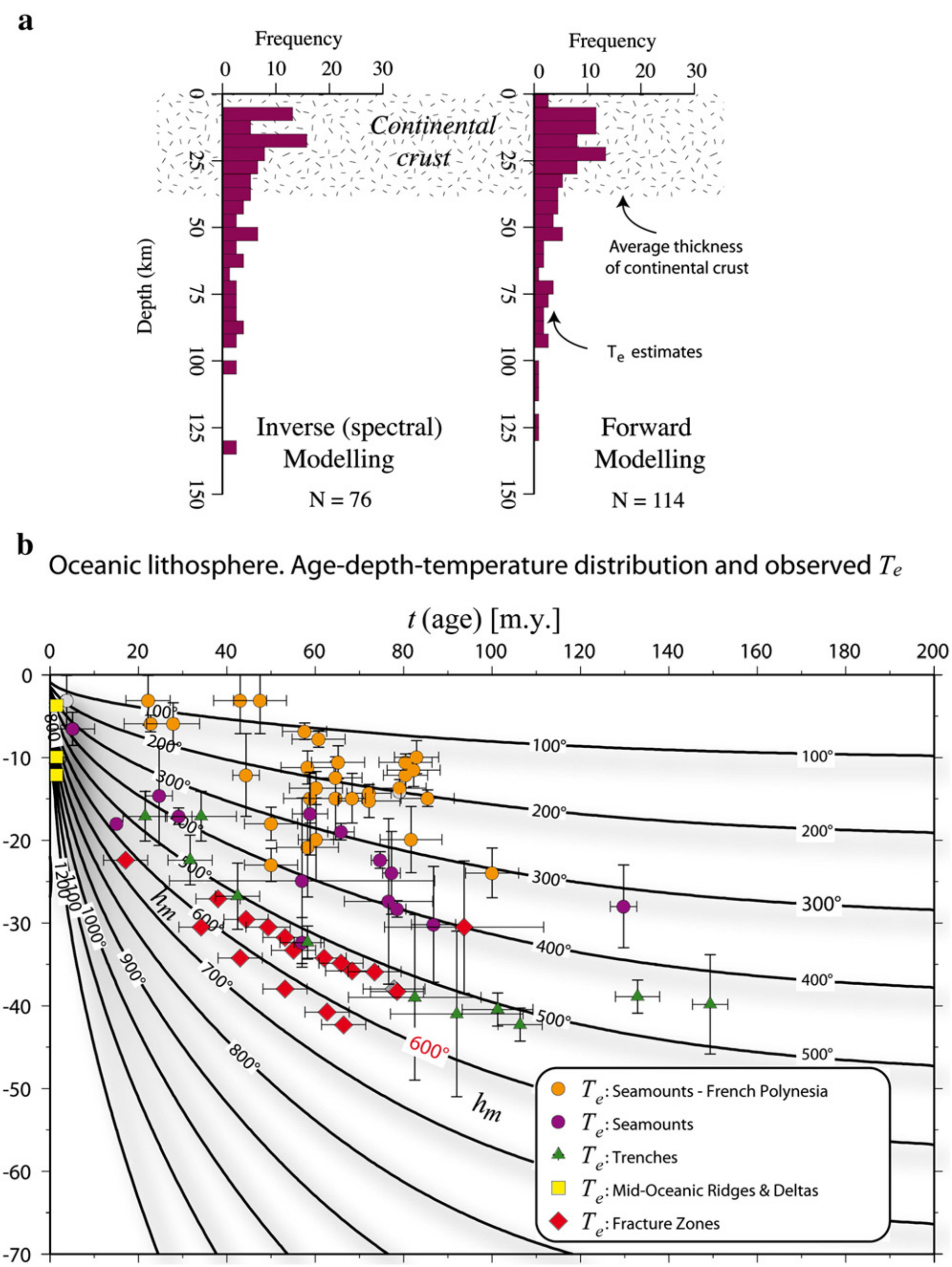

Fig. 2. a. Histograms showing continental T_e estimates based on forward and inverse (i.e. spectral) gravity anomaly modelling methods. The histograms are based on data in Tables 5.2 and 6.2b of Watts (2001) and references therein. The two methods yield similar results and show that continental lithosphere is characterised by both low and high T_e values. The presented T_e values reflect a mix of loading situations. The spectral estimates include continent-wide and local studies and reflect mainly shields, but include orogens and rifts. The forward estimates mainly refer to foreland basins and rifts but also include shields. In general, the low T_e come from orogens and rifts and the high T_e — from shields. Modified from Burov and Watts (2006). b. Revealed correlation between the observed flexural strength T_e and age–temperature of the oceanic lithosphere. Thermal distribution is computed according to the plate cooling model (Parsons and Sclater, 1977; Burov and Diament, 1995). The T_e data are superimposed with computed geotherms. The relevant estimates refer to zones with normal thermal gradient such as fracture zones and trenches. Naturally, the cases of seamount loading cannot be fitted with the standard cooling model due to local thermal rejevenation of the underlying lithosphere by hot-spot activity. However, locally-tuned thermal models confirm T_e correlation with the depth of the geotherm 400–500 °C, specifically for seamounts older than 10 Myr (Watts, 2001).

T_e values that were significantly smaller than those derived from forward modelling (see Cochran, 1980 and references therein). The subsequent development of more robust methods of determining T_e using a Bouguer coherence method (e.g. Forsyth, 1985; Lowry and Smith, 1994), however, has yielded values more compatible with forward modelling (Fig. 2a).

It is noteworthy that what we call above inverse methods are classical admittance or coherence inversion methods. These are done assuming a homogeneous and continuous plate (which is not necessary in case of direct models). In addition, with coherence, one assumes that surface and inner loads are uncorrelated, while admittance method needs flat surface topography, and care must be taken not to incorporate regions of active deformation when estimating the T_e of continental plates (e.g., Crosby, 2007). Strictly speaking, these simplifying assumptions are not compulsory in case of spectral interpretation in general. Yet, in the oceanic domain, these approximations are quite reasonable and often direct models also assume the same setup (e.g., Diament and Goslin, 1986). Therefore with the same mechanical model, if properly formulated, spectral-based and direct models must give identical results.

3. Plate flexure and rheology

The lithosphere responds to normal surface and subsurface loads by bending. Bending is characterized by vertical deflection, $w(x)$ and local radius of curvature, $R_{xy}(x)$ or curvature, $K(x)=-R_{xy}^{-1}=\partial^2 w/\partial x^2$. The amplitude and wavelength, λ, of bending depend on the flexural rigidity D or equivalent elastic thickness T_e ($D=ET_e^3(12(1-\nu^2))^{-1}$). The flexural equation, when written in the form with bending moment $M_x(x)$ in the flexural term, is rheology independent. The elasticity is not inherent to this equation but is used as a simplest rheological interpretation of the bending strength. T_e and D are estimated by fitting the observed flexural profiles (Moho depression for continents or bathymetry for oceans) to the solution of thin plate equation (e.g., Timoshenko and Woinowsky-Krieger, 1959; Burov and Diament, 1992):

$$\frac{\partial^2}{\partial x^2}\left(\overbrace{\underbrace{\frac{ET_e^3}{12(1-\nu^2)}}_{D(x)}\underbrace{\frac{\partial^2 w(x)}{\partial x^2}}_{K(x)}}^{M_x}\right)+\frac{\partial}{\partial x}\left(F_x\frac{\partial w(x)}{\partial x}\right)+\Delta\rho g w(x) = \rho_c g h(x)+p(x) \quad (1a)$$

where F_x is horizontal fiber force, $\Delta\rho$ is the density contrast between surface material (topography/sediment) and asthenosphere, ρ_c is the density of surface material, $h(x)$ is topography elevation and $p(x)$ is additional surface or subsurface load. For inelastic plates, T_e and D have sense of "condensed" plate strength linked to the integrated plate strength B.

For example, for a single-layer plate of thickness h_m with $T_e=T_{e\_ocean}$:

$$B=\int_0^\infty \sigma_{xx}^f(x,y,t,\dot{\varepsilon})dz \quad \text{while} \quad (1b)$$

$$T_{e\_ocean}=\left(12\left(\frac{\partial\sigma_{xx}}{\partial y}\right)^{-1}\int_{-\frac{h_m}{2}}^{\frac{h_m}{2}}\sigma_{xx}^f z dz\right)^{\frac{1}{3}};\ T_{e\_ocean}<h_m$$

where σ_{xx}^f is horizontal stress (bending stress in case of flexure) (Burov and Diament, 1995). T_e is therefore a direct proxy for the long-term integrated strength of the lithosphere, B (see Watts, 2001). For inelastic rheology, T_e is smaller than the mechanical plate thickness (h_m) and has no geometrical interpretation but is derived from the rigidity D and the flexural moment M. M and D are obtained from depth integration of bending stress σ_{xx}^f, which is a function of local plate curvature $K(x)=\partial^2 w/\partial x^2$ (e.g., Burov and Diament, 1995):

$$\begin{aligned}&\sigma_{xx}^f(z,K)\approx\min(\sigma^b(z),\sigma^v(z),K(z-z_n(K))E(1-\nu^2)^{-1})\\&D(x,K)=\left|\frac{M(x,K)}{K}\right|\\&T_e(x,K)=\left(M(x,K)\frac{12(1-\nu^2)}{EK}\right)^{\frac{1}{3}}\end{aligned} \quad (2a)$$

$$\begin{cases}\sigma_{ij}^e=\lambda\varepsilon_{ii}\delta_{ij}+2G\varepsilon_{ij}\\ \tau^b=C_0+\tan(\phi)\sigma_n\\ \tau_{ij}^v=(\dot{\varepsilon}_{ij}^d A^{-1})^{1/n}e^{H(nRT)^{-1}}\end{cases} \quad (2b)$$

Here $z_n(K)$ is the "floating" depth to the neutral stress free plane: $z_n(K)\rightarrow 0.5h_m$ as $K\rightarrow 0$, $\sigma^b(z)$, $\sigma^v(z)$ are brittle and viscous–ductile yield strength at depth z, respectively. Eq. (2b) refer to the rheological constitutive laws. Repeating indexes mean summation and δ is Kronecker's operator. Superscripts "e", "b", and "v" refer to the elastic, brittle, viscous–ductile constitutive laws, respectively. λ and G are Lame's constants. τ is shear and σ_n is normal stress on the brittle shear band or fault surface, C_0 is cohesion, ϕ is internal friction angle, $\dot{\varepsilon}_{ij}^d$ is ductile strain rate, n is power-law exponent, A is material constant, H is enthalpy of creep activation, R is gas constant, T is temperature in K (see also Table 1). By comparing observations of flexure in the regions of long-term surface loading such as ice, sediment and volcanoes, to the predictions of simple elastic plate models, it has been possible to estimate T_e and thus B, in a wide range of geological settings. Oceanic flexure studies suggest that T_e is in the range 2–40 km and depends on load and plate age (Fig. 2a,b). These results are consistent with the predictions of rock mechanics, so that T_e values follow the age-controlled depth to 400–500 °C (Fig. 2b). The Brace–Goetze YSEs (Goetze and Evans, 1979; Brace and Kohlstedt, 1980) predict that strength should increase until the depth of the brittle–ductile transition (BDT), and then decrease in accordance with the brittle and ductile deformation laws. In oceanic regions, the failure curves are approximately symmetric about the BDT where the brittle-elastic and elastic-ductile layers contribute equally to the strength. Since both T_e and BDT generally exceed the mean thickness of the crust (~7 km) there is a little doubt that the largest contribution to the strength of oceanic lithosphere comes from the mantle, not the crust.

McAdoo et al. (1985) used Eqs. (2a) and (2b) to calculate the ratio of $T_e(K)$ to h_m for the middle value of oceanic thermal age of 80 Ma, a dry olivine rheology, and a strain rate of $10^{-14}\,s^{-1}$. They showed that for low curvatures (i.e. $K<10^{-8}\,m^{-1}$) the ratio is 1, indicating little difference between the elastic thickness values. However, as curvature increases, the ratio decreases as $T_e(K)$ decreases. For $K=10^{-6}\,m^{-1}$ the ratio is ~0.5, indicating a 50% reduction in the elastic thickness.

The tendency of the oceanic lithosphere to yield in the seaward walls of trenches can be understood in terms of simple mechanical considerations. Ideal elastic materials support any stress level. In the case of real materials, stress levels are limited by rock yield strength at corresponding depth, or more exactly, at corresponding P–T conditions. Flexural strain in a bending plate increases with distance from the neutral plane. Consequently, the uppermost and lowermost parts of the plate are subject to higher strains and may experience brittle or ductile deformation as soon as the strain cannot be supported elastically. These deformed regions constitute zones of mechanical weakness since the stress level there is lower than it would be if the material maintained elastic behaviour and,

Table 1

Summary of thermal and mechanical parameters used in model calculations

Thermal	Surface temperature (0 km depth)	0 °C
	Temperature at the bottom of thermal lithosphere	1330 °C
	Thermal conductivity of crust	2.5 Wm^{-1} $°C^{-1}$
	Thermal conductivity of mantle	3.5 Wm^{-1} $°C^{-1}$
	Thermal diffusivity of mantle	10^{-6} m^2 s^{-1}
	Radiogenic heat production at surface	9.5×10^{-10} W kg^{-1}
	Radiogenic heat production decay depth constant	10 km
	Thermo-tectonic age of the lithosphere	150 (Fig. 1b) and 500 (Fig. 1c) Myr
Mechanical	Density of upper crust	2700 kg m^{-3}
	Density of lower crust	2900 kg m^{-3}
	Density of mantle	3330 kg m^{-3}
	Density of asthenosphere	3310 kg m^{-3}
	Lamé elastic constants λ, G (here $\lambda = G$)	30 GPa
	Byerlee's law — friction angle	30°
	Byerlee's law — cohesion	20 MPa

Summary of ductile parameters used in model calculations*

	Composition	Pre-exponential stress constant A MPa^{-n} s^{-1}	Power law exponent n	Activation energy, Q KJ mol^{-1}	Fig. 1
Upper crust	Wet quartzite	1.1×10^{-4}	4	223	b
Lower crust	Dry Columbia diabase	190 ± 110	4.7 ± 0.6	485 ± 30	
	Dry Maryland diabase	8 ± 4	4.7 ± 0.6	485 ± 30	c
	Undried Pikwitonei granulite	1.4×10^4	4.2	445	b
Mantle	Dry olivine	4.85×10^4	3.5	535	b, c (jelly sandwich)
	Wet olivine	417	4.48	498	b, c (crème-brûlé)

* The failure envelopes in this paper match those in Jackson (2002). The Jackson (2002) envelopes are based on Fig. 4 in Mackwell et al. (1998) who did not list all parameters, referring instead to the primary references. We therefore list the parameters that we have used here.

importantly, there stress is lower than it would be on the limits of the elastic core that separates the brittle and ductile regions. The level of the brittle and ductile stress, however, is not zero. A load emplaced on the oceanic lithosphere will therefore be supported partly by the strength of the elastic core and partly by the brittle and ductile strength of the plate. The significance of T_e that has been estimated at trenches is that it reflects this combined, integrated, strength of the plate.

McKenzie and Fairhead (1997) argue that most previous continental T_e estimates based on the Bouguer coherence (spectral) method are over-estimates rather than true values. They used a Free-Air admittance method to argue that continental T_e was low, <25 km. Since their estimates of the elastic thickness were comparable to the seismogenic layer thickness, T_s, they proposed that the strength of the continental lithosphere resides in the crust, not the mantle.

In particular, Jackson (2002) has concluded that T_e of the Indian plate should not exceed 30 km thus justifying the assertion that plate strength in concentrated in the crust. As mentioned, FAA admittance models may become unreliable in continental domain since they are technically not suited for the areas of actively deforming elevated topography (e.g., Crosby, 2007). For this reason Jackson (2002) has limited his reflectively repeated flexural profiles to forelands of Himalaya (Fig. 3). Formulated this way, no model, forward or inverse, can produce correct results, since in Himalayas, as was shown by Molnar and Lyon-Caen (1988) or Jin et al. (1994), the mountain loads, tectonic boundary forces and moments provide major contribution to the observed large-scale gravity signatures at very long (many hundred kilometers) distances from the mountain range. If these loads and forces are ignored, any flexural model will provide largely underestimated T_e values, specifically in case of inverse models that inherently assume reflecting or repetitive boundary conditions. Indeed, the gravity signal observed in the foreland is largely affected by mountain and plate-end loading and has little to do with the local topography load. We have tested this hypothesis by running robust forward flexural models. The tested profiles include Jackson's (2002) profiles but are extended to the north and south to include the Himalaya and the entire Indian plate. The optimal fit to the gravity is obtained by varying T_e and flexural moment at the end of the plate ($10^{16}-3\times10^{17}$ N m/m, same range as in Molnar and Lyon-Caen, 1988; Jin et al., 1994; Burov and Watts, 2006). The results (Fig. 3) are compatible with the previous forward flexural models and show that: (1) over the elevated topography, both Bouguer and FAA gravity signals associated with flexure of the Indian plate provide a best fit to the data for T_e values on the order of 60 to 90 km (all these values are larger than the crustal thickness of the Indian lithosphere); (2) over the forelands, in the area analyzed by Jackson (2002), the gravity anomalies predicted by the for T_e values ranging from 30–40 km to 80–90 km fit almost equally well, or equally bad, the observations. The signal in this area is weak and includes substantial regional component, which explains the bias in the results of Jackson (2002) toward the smallest T_e values. However, in the area of strong gravitational and topography signal directly affected by the mountain load, the best fit is obtained for high T_e values on the order of 60 to 80 km, whatever anomaly is used, Bouguer or FAA. As can be seen from Fig. 3, in contrary to what is stated by Jackson (2002) and McKenzie and Fairhead (1997), Bouguer and FAA based models produce identical results for T_e if similarly formulated in terms of boundary conditions, topography and subsurface loads.

We conclude that the "problem" of "low continental T_e " most probably does not exist: the reduced T_e values obtained from some inverse gravity models is an artefact stemming from mechanically inconsistent formulation of the flexural problem in the continental domain. The FAA admittance models (Jackson, 2002; McKenzie and Fairhead, 1997) did not include main topography loads but considered that the modelled flexure is not affected by the presence of the topography and plate boundary loads. This is incorrect and leads to arbitrarily underestimated predictions for the effective elastic thickness.

As mentioned (see also Burov and Watts, 2006 and Fig. 2a), tests with synthetic and observed gravity anomaly and topography data show, that when the Bouguer coherence and Free-Air admittance methods are similarly formulated, they yield the same results: namely that continental T_e ranges from a few km to >70 km and that it varies spatially over relatively short (~100 km) horizontal scales (Pérez-Gussinyé and Watts, 2005).

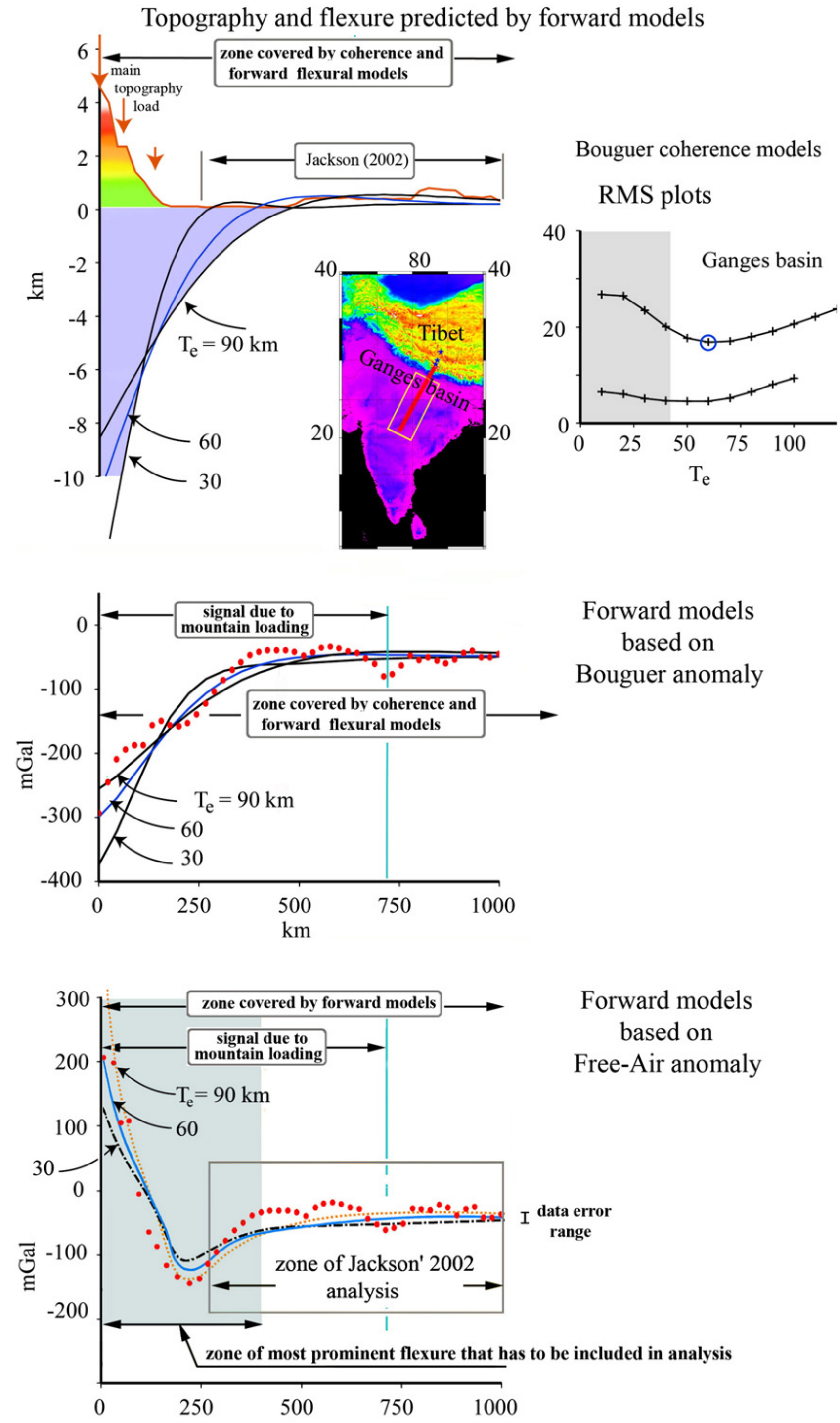

Fig. 3. Comparison of observed (GETECH (UK) SEAGP gravity data) and calculated Bouguer gravity and Free-Air anomalies along a profile of the Himalayan foreland at about longitude 80° E, which includes the zone of FAA-admittance analyis of (Jackson, 2002). As can be seen, flexure in the northern part of Jackson's (2002) profile is must be affected by mountain loading which was not accounted in his model (the reason why this model could produce correct results for whatever method used). In isostatic models, the acceptable error for long-wavelength data misfit should be no worth than 5–10 mGal for amplitude and <10% for wavelength. The calculated profile is based on a discontinuous (i.e. broken) elastic plate model, a load comprising both the topography (density = 2650 kg m^{-3}) above sea-level between the Main Boundary Thrust (MBT) and plate break (grey shaded region) and the material (density = 2650 kg m^{-3}) that infills the flexure (density = 2650 kg m^{-3}), a mantle density of 3330 kg m^{-3} and T_e of 70 km. Jordan and Watts (2005) have shown that this combination of load geometry and T_e provide the best overall fit to the observed Bouguer anomaly. The dashed thin blue line shows the calculated Bouguer anomaly for the load shown and T_e = 30–40 km, which is the value preferred by McKenzie and Fairhead (1997). This value does not, however, explain the amplitude and wavelength of the Bouguer anomaly because the amplitude misfit is 20–50 mGal in the area of interest (i.e., Himalaya and the foredeep basin, where the signal is most informative and robust), whereas the predicted wavelength is twice shorter than that of the signal. Similar results are obtained for Free-Air anomaly forward models shown on the bottom: in the area of most reliable signal, the best FAA fit is for T_e = 80–90 km, the worst — for T_e below 30 km. In the area used by Jackson (2002), all tested T_e values predict very similar gravity signal due smoothed plate deflection cased by the remote Himalayan load and the absence of significant local topographic loading.

Indeed, the characteristic length-scale of flexural loading is expressed via flexural parameter (Turcotte and Schubert, 2002), α:

$$\alpha \sim T_e^{3/4}\left(E(3(1-\upsilon^2)\Delta\rho g)\right)^{1/4} \approx 48.5T_e^{3/4} \tag{3}$$

This parameter characterizes the distance (2α–3α) at which the plate deflection associated with a given point load will become negligible. For T_e of 30 km such distance would be about 250–400 km, for T_e of 40 km to about 300–400 km, for T_e of 90 km to 500–700 km. Profiles modelled by Jackson (2002) and McKenzie and Fairhead (1997) stop at 250 km from the axis of Himalayan mountain range. The model of Jackson (2002) is formulated under assumption that the influence of Himalaya (or any other elevated topography in McKenzie and Fairhead, 1997) is negligible for their area of analysis. Consequently, these models "technically" cannot yield T_e values larger than 30–40 km. This provides a mechanical explanation of the underestimated T_e values obtained from FAA admittance models of Jackson (2002) and McKenzie and Fairhead (1997) as well as from other models that used similar model setup and method.

While T_e values that exceed the local thickness of the crust do not indicate which layer, crust or mantle, is strong (Burov and Diament, 1995, 1996; Burov, 2007), they are indicative of high mantle strength. For example, the Bouguer anomaly associated with the flexure of the Indian shield beneath the Ganges foreland basin by the Himalaya requires a T_e of ~70 km (between 60 and 90 km: e.g. Fig. 3) which is significantly higher than the local crustal thickness of ~40 km. These estimates are consistent with previous forward and spectral flexural models of the area that considered a gravitationally and mechanically consistent problem, i.e. included the entire loading domain: Indian Plate, Himalaya and Tibet (e.g., Lyon-Caen and Molnar, 1983, 1984; Jin et al., 1994; Caporali, 1995, 2000; Jordan and Watts, 2005). It is difficult using the Brace–Goetze failure envelopes to explain such high values without invoking a significant contribution to the strength from the sub-crustal mantle.

Irrespective of the different methodologies that have been used, it is clear from Figs. 2 and 3 that continental T_e values can be high and may well exceed not only the seismogenic layer thickness, T_s, which is usually located in the upper crust (i.e. ~20 km) but also the total crustal thickness. We are not surprised by this result. T_e reflects, we believe, the long-term integrated strength of the lithosphere while T_s is representative of the strength of the uppermost of the crust on short-time scales. It is difficult to use the failure envelopes to predict the actual depth to which seismicity should occur. However, if we assume that Byerlee's law is applicable to great depths, then the BDT increases from 15 to 25 km for the relatively low strain rates of flexure to 50–70 km for the relatively high seismic strain rates. We attribute the general absence of mantle earthquakes at these latter depths to the lack of sufficiently large tectonic stresses (>2 GPa) to generate sliding.

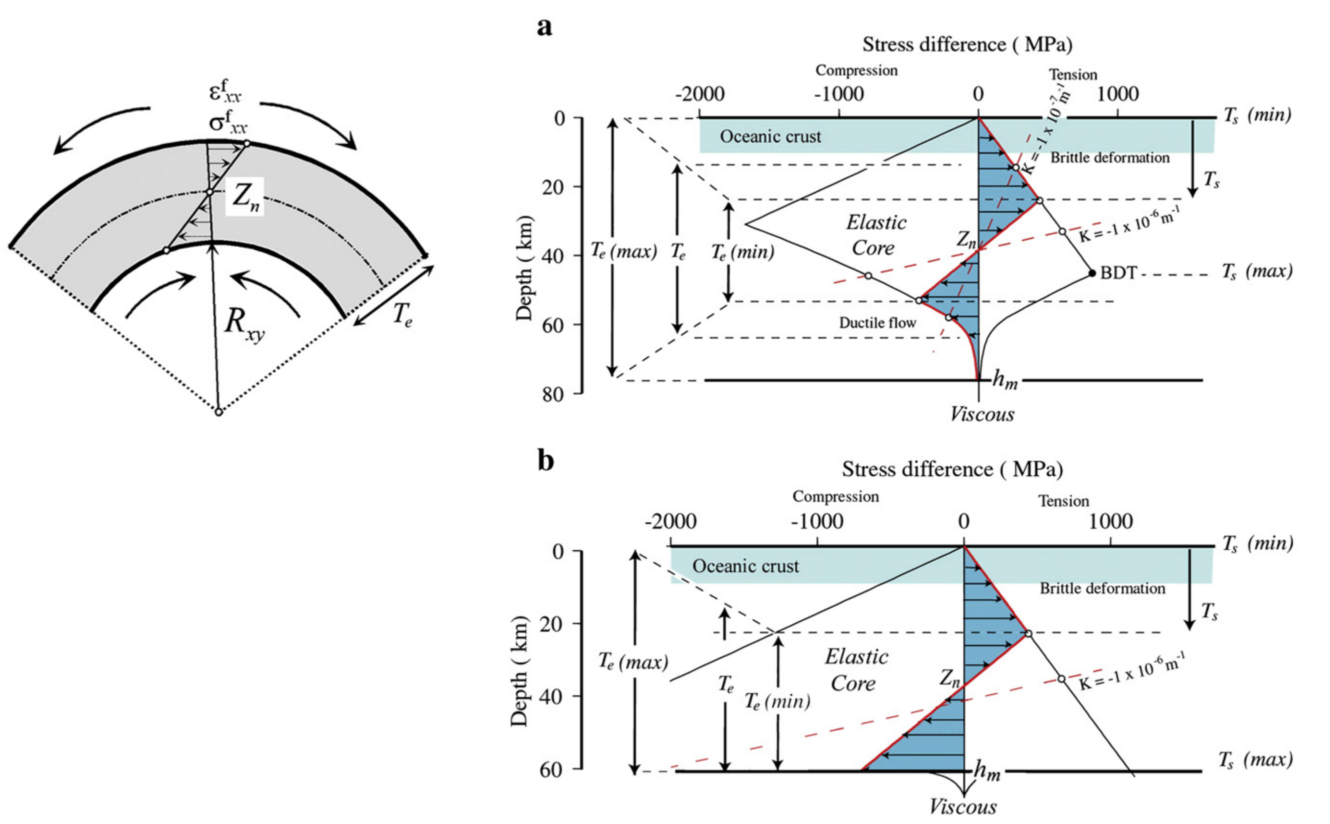

Fig. 4. a. T_e and T_s for an idealised case of flexure of the oceanic lithosphere. Thin solid line shows the Yield Strength Envelope (YSE) for 80 Ma oceanic lithosphere. The brittle behaviour is described by Byerlee's law, the ductile behaviour by an olivine power law (stress constant, A, of 7×10^{-14} $Pa^{-3}\,s^{-1}$; creep activation energy, Q, of 512 kJ/mol (Kirby and Kronenberg, 1987) and, the thermal structure by the cooling plate model (Parsons and Sclater, 1977). Thick solid line shows the stress difference for a load which generates a moment, M, of 2.2×10^{17} N m^{-1} and curvature, K, of 5×10^{-6} m^{-1}. The figure shows that the load is supported partly by a strong elastic layer or 'core' and partly by the brittle and ductile strength of the lithosphere. The dashed lines show the cases of K of 1×10^{-7} m^{-1} and 1×10^{-6} m^{-1} which bracket the range of observed values at deep-sea trench–outer rise systems (Goetze and Evans, 1979; McNutt and Menard, 1982; Burov and Diament, 1992). The figure shows that T_s corresponds to the depth of the intersection of the moment–curvature curve with the brittle deformation field, but could extend from the surface, T_s (min), to the Brittle Ductile Transition (BDT), T_s (max). T_e, in contrast, could extend from the thickness of the elastic 'core', T_e (min), to the thickness of the entire elastic plate, T_e (max). Both T_s and T_e depend on the moment generated by the load and, hence, the plate curvature. b. YSE based on "Crème brulée" rheology model: interpretation of the seismogenic layer, T_s and equivalent elastic thickness, T_e, under assumption of Jackson (2002) that the mechanical strength of the lithosphere is concentrated in the brittle layer. This case considers brittle-elastic lithosphere with zero strength ductile part, for the same typical amount of flexure ($K=5\times10^{-6}$ m^{-1}) and T_s value (20 km) as in the case shown in panel a. The figure demonstrates inconsistence of two simultaneous assumptions: of weak ductile mantle and $T_e=T_s$, due to geometric incompatibility between seismogenic layer (T_s) and elastic thickness (T_e). If $T_s=20$ km than $T_e>40$ km.

4. T_e and T_s: Insights from flexural mechanics

While T_e and T_s are similar in the oceans and in some continents, we believe that they have fundamentally different meanings. Seismicity refers to short-term elastic or at best elasto-plastic deformation. It has not relation to the ductile strength of rocks because geological-scale ductile creep cannot be activated at seismic strain rates. T_s reflects the strength of, or more precisely the stress level in, the uppermost brittle layer of the lithosphere while T_e is indicative of the strength of the elastic portion of the lithosphere that supports a particular load and, importantly, the brittle and ductile strength of the entire elastic layer. The difference is most obvious in unflexed lithosphere when T_s is zero and T_e takes on its highest possible value (Burov and Diament, 1995, Fig. 4). Differences persist into flexed lithosphere where T_e slowly decreases with increasing curvature and, hence, bending stress (McNutt and Menard, 1982; Chen and Molnar, 1983) while T_s simply reflects the local stress level. Yield Strength Envelope (YSE) considerations (e.g. Fig. 4a) suggest that in case of oceanic lithosphere, with its single-layer rheology, the BDT just happens to fall approximately mid-way in the strong elastic portion of the lithosphere. Therefore, the values of T_e and T_s may well be close. However, if the ductile part of the lithosphere mantle is mechanically weak (Fig. 4b), two simultaneous assumptions of weak ductile mantle and $T_e = T_s$, become impossible due to the incompatibility between the seismogenic layer (T_s) and elastic thickness (T_e) in this case (for example, if $T_s = 20$ km then T_e must be 40 km). Thus CB rheology is incompatible with the assumption $T_e = T_s$.

These conclusions are in accord with observations at deep-sea trench–outer rise systems. Because of the high curvatures that are experienced by the oceanic lithosphere as it approaches a trench, T_e is less than it would otherwise be on the basis of plate age because of yielding. Judge and McNutt (1991), for example, have shown that in the high curvature region of the seaward wall of the northern Chile trench (curvature, $K = 1.3 \times 10^{-6}\,\mathrm{m}^{-1}$) T_e is 22 ± 2 km, which is less than the T_e of 34 km that these workers expected on the basis of the thermal age of the subducting oceanic lithosphere.

Fig. 5 compares T_e and T_s at northern Chile as well as other different deep-sea trench–outer rise systems in the Pacific and Indian oceans. The figure shows that T_e and T_s are similar, at least for ages of the oceanic lithosphere ≤ 100 Ma. For greater ages, there is a suggestion of a 'threshold' beyond which T_e exceeds T_s. This is attributed to the fact that as the lithosphere ages, its strength increases, and so the curvature and, hence, the bending stress associated with the same load decreases. Therefore, T_e, which mainly reflects the integrated strength of the lithosphere, increases while T_s, which depends more directly on the stress level, decreases. It is noteworthy that, due to the linear

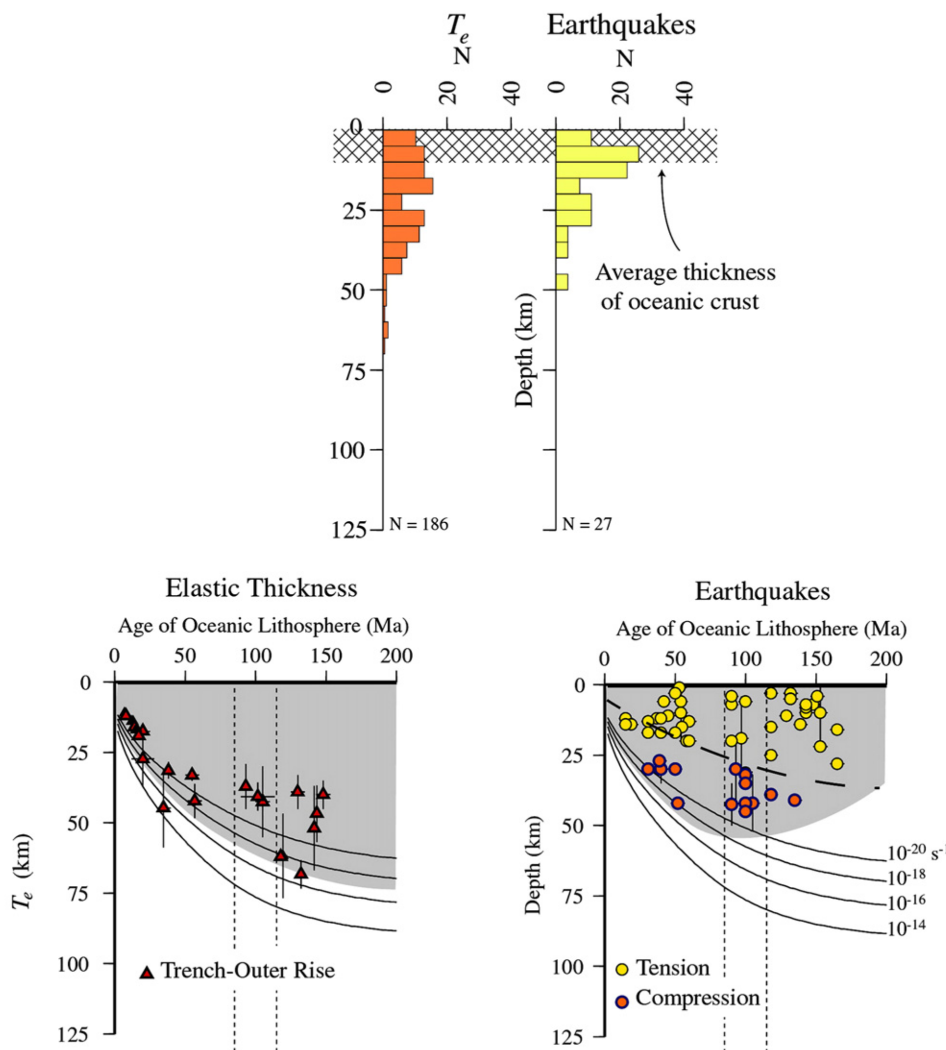

Fig. 5. This figure compares T_e and T_s at northern Chile as well as other different deep-sea trench–outer rise systems in the Pacific and Indian oceans. The figure shows that T_e and T_s are similar, at least for ages of the oceanic lithosphere ≤ 100 Ma. For greater ages, there is a suggestion of a 'threshold' beyond which T_e exceeds T_s. This is attributed to the fact that as the lithosphere ages, its strength increases, and so the curvature and, hence, the bending stress associated with the same load decreases. Therefore, T_e, which mainly reflects the integrated strength of the lithosphere, increases while T_s, which depends more directly on the stress level, decreases. Modified from Burov and Watts (2006).

dependence of the brittle strength on the total confining pressure (Byerlee, 1978), the brittle strength is considerably (2–3 times) higher in case of concave downward flexure (= upper layer compression, Fig. 4), and smaller in case of concave upward flexure (upper layer tension, Fig. 4). These results in the observed considerable differences between the T_s depths in case of tensional and compressional earthquakes (Fig. 5). The great dependence of T_s on the intra-plate stress level thus supports our assertion that T_s cannot be simply related to T_e.

We have based the discussion thus far on a YSE that only considers the stresses generated in a flexed plate by bending. We have not, therefore, taken into account the effect of any in-plane stresses that act on the plate due, for example, to tectonic boundary loads. It is difficult to conceptualise T_e and T_s from a YSE in the presence of such stresses. However, we can say that T_s will be conditioned by the brittle failure due to these stresses and, as a consequence, will be even less related to the bending stress and, hence, the local T_e.

As for the oceans, T_e data is a main proxy for long-term strength of continental lithosphere. In continents, T_e ranges from 0 to 110 km and shows only partial relationship with age. Although the continental lithosphere should strengthen while getting colder with time (Fig. 6), there is no such a clear T_e-age dependency in continents as in oceans (Fig. 2b). Many plates underwent thermal events that changed their thermal state in a way that it does not correlate with their geological age (e.g., Kazakh shield, Burov et al., 1990; Adriatic lithosphere, Kruse and Royden, 1994). On the other hand, after 400–750 Ma (Fig. 6) temperature distribution in the lithosphere approaches stationary state and does not evolve with age. As mentioned, interpretation of the surface heat flux in continental domain is ambiguous because of uncertain crustal heat generation and thermal effects associated with erosion, sedimentation and climatic changes (Jaupart and Mareschal, 1999). Surface heat flow mainly reflects crustal processes and should not be used to infer the subcrustal geotherm (England and Richardson, 1980).

The base of the mechanical lithosphere in continents, h_m, is referred to isotherm of 700–750 °C below which the yielding stress is less than 10–20 MPa. The background strain rates are typically known within one order of magnitude accuracy. As can be seen from Fig. 7b, such uncertainty is acceptable, since it affects the yield limits no more than by 10%.

The rheological meaning of T_e in the continents is not as clear as it is in the oceans (Fig. 6). The T_e data show a bimodal distribution (Fig. 2a), with low values clustering at 30–40 km, and high values clustering at 80 km (Burov and Diament, 1995; Watts, 2001). The reason for this clustering probably refers to the influence of plate structure: depending on the ductile strength of the lower crust, the continental crust can be mechanically coupled or decoupled with the mantle resulting in highly differing T_e. Burov and Diament (1992) have shown for "typical" continental lithosphere, that the weak ductile zones in the lower crust do not allow flexural stresses to be transferred between the strong brittle, elastic or ductile layers of the jelly "sandwich". As result, there are several "elastic" cores inside the bending plate. In such a multilayer plate stress levels are reduced, for

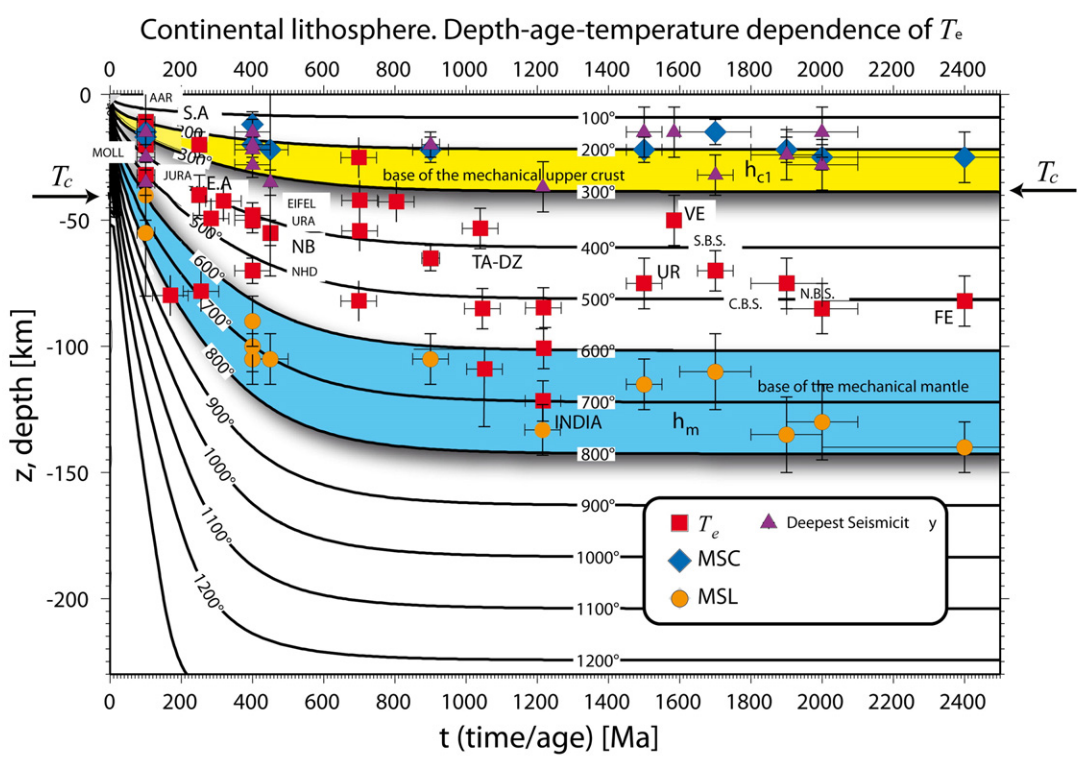

Fig. 6. Compilation of observed elastic thickness (T_e) against age of the continental lithosphere at the time of loading and the thermal model of the continental lithosphere (equilibrium thermal thickness, $a = z(1330\ °C)$, of 250 km (Appendix B). Also shown is the depth to the mechanical base of the lithosphere and maximal depths of seismicity (where available). The data refer to the studies that have taken into account – at minimum – surface topography loads. Where available, we preferred estimates based on robust forward models rather than possibly less reliable spectral estimates (Lowry and Smith, 1994; Watts and Burov, 2003; Jordan and Watts, 2005; Burov and Watts, 2006; Burov, 2007). The lines are isotherms with account for radiogenic heat production in the crust. Filled squares are estimates of T_e in collision zones (foreland basins, thrust belts); filled circles correspond to post-glacial rebound data. Isotherms 250 °C–300 °C mark the base of the mechanically strong upper crust (quartz). The isotherms 700 °C–750 °C mark h_m, the base of the competent mantle (olivine). Note that there is no significant changes in the thermal structure of the lithosphere after ~750 Ma, though there are significant reductions in T_e even for these ages. These reductions are obviously caused by differences in crustal structure and rheology. The notations are: Foreland basins/mountain thrust belts data: E.A — Eastern Alps; W.A. — Western Alps; AD — Andes (Sub Andean); AN — Apennines; AP — Appalachians; CR — Carpathians; CS — Caucuses; DZ — Dzungarian Basin; HM — Himalaya; GA — Ganges; KA — Kazakh shield (North Tien Shan); KU — Kunlun (South Tarim); NB — North Baikal (chosen since this part of the Baikal rift zone is believed to represent a "broken" rift currently dominated by flexural deformations); TA — Central and North Tarim; PA — Pamir; TR — Transverse Ranges; UR — Urals; VE — Verkhoyansk; ZA — Zagros. Post—glacial rebound zones: L.A. — lake Algonquin; FE — Fennoscandia; L.AZ — lake Agassiz; L.BO — lake Bonneville; L.HL — lake Hamilton. Data sources: S.A., AN., CR., HM, NB, KA, TA, PA,KU, GA, AD, TA, W.A, E.A., DZ, AP, GA,TR,VE,FE: (Burov and Diament, 1995 and references therein). Other data sources (ZA, L.A., L.AZ, L.BO, L.HL): (Watts, 1992, 2001).

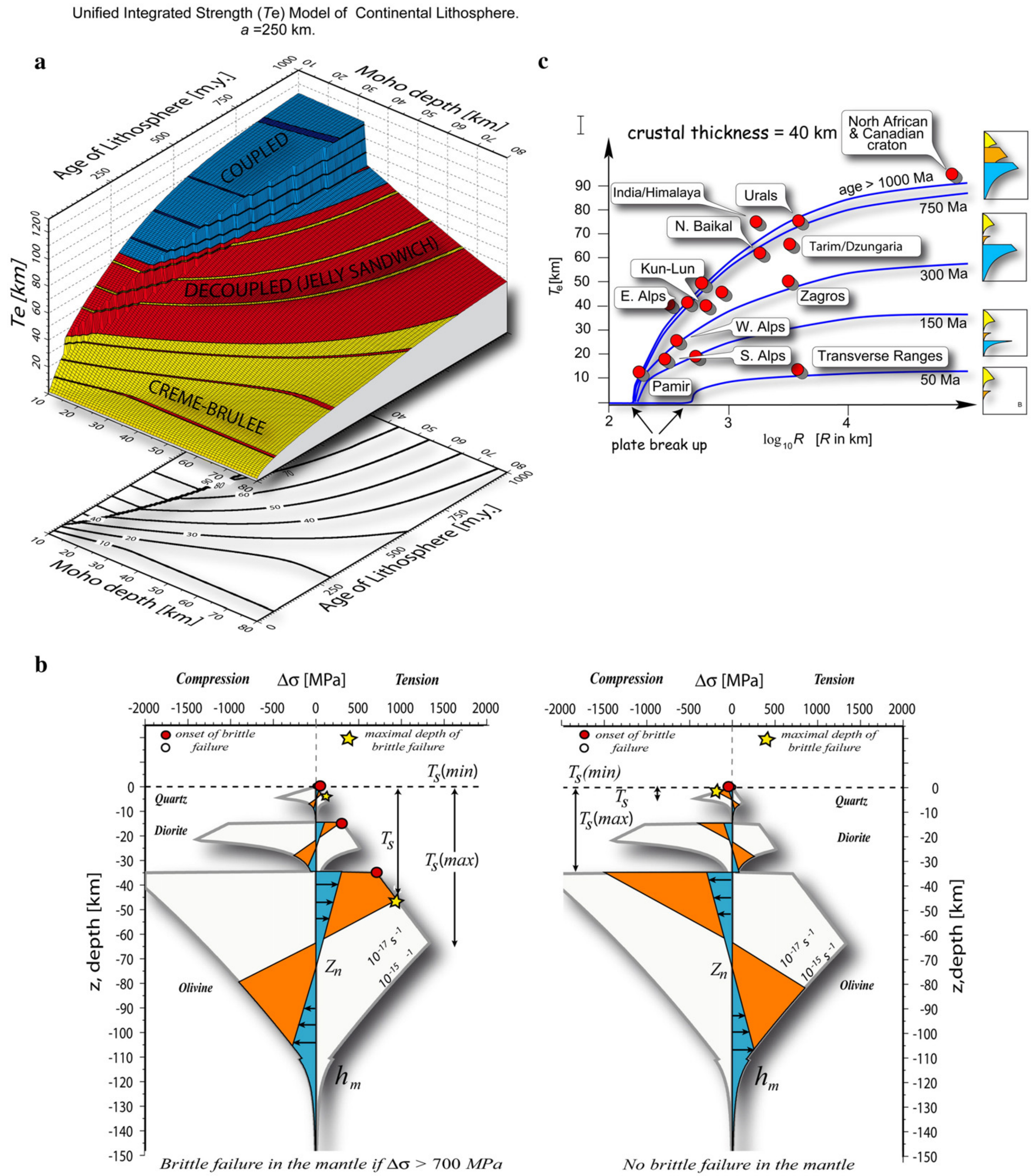

Fig. 7. Predicted relationships between the rheology structure, age, plate curvature K, T_e and T_s for continental lithosphere. a. Unified model of flexural strength of lithosphere, computed for dry quartz upper crust, quartz–diorite lower crust, dry olivine mantle (Table 1). Equilibrium thermal thickness of the lithospheres, $a = 250$ km. After Burov and Diament (1996) and Burov (2007). b. Stress distribution within continental YSE for concave upward and concave downward flexure (see text). c. Predicted dependence of continental T_e on age and curvature of the lithosphere, computed for normal crustal thickness, T_c, of 40 km and compared with the data for continental plates with normal crustal thickness. Right: geometry of corresponding YSEs (same lithosphere structure and composition as in Fig. 7a). Modified (extended) from Burov and Diament (1996). d. T_e and T_s as function of curvature in a two-layer classical "jelly sandwich" plate (strong upper crust, weak lower and intermediate crust, strong mantle). After Burov and Watts (2006). e. T_e and T_s as function of curvature in a three layer plate (strong upper crust, strong lower or intermediate crust, strong mantle). After Burov and Watts (2006). f. Relationships between the plate curvature, T_e and T_s for different ages of the lithosphere. Left: assumption of equilibrium thermal thickness of the lithosphere, $a = 250$ km. Right: $a = 125$ km. Black curves are for decoupled rheology, grey curves are for coupled rheology.

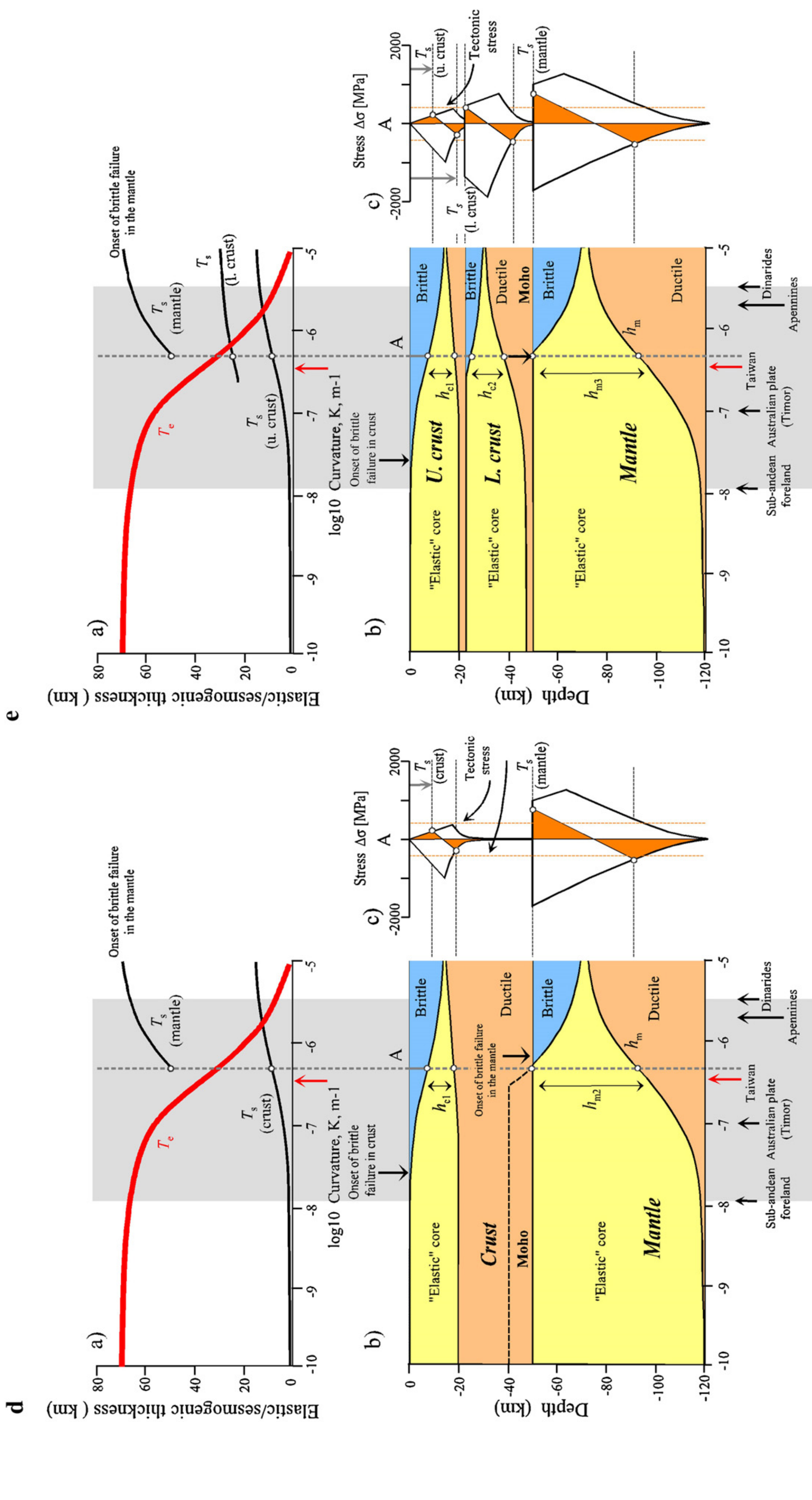

Fig. 7 (continued).

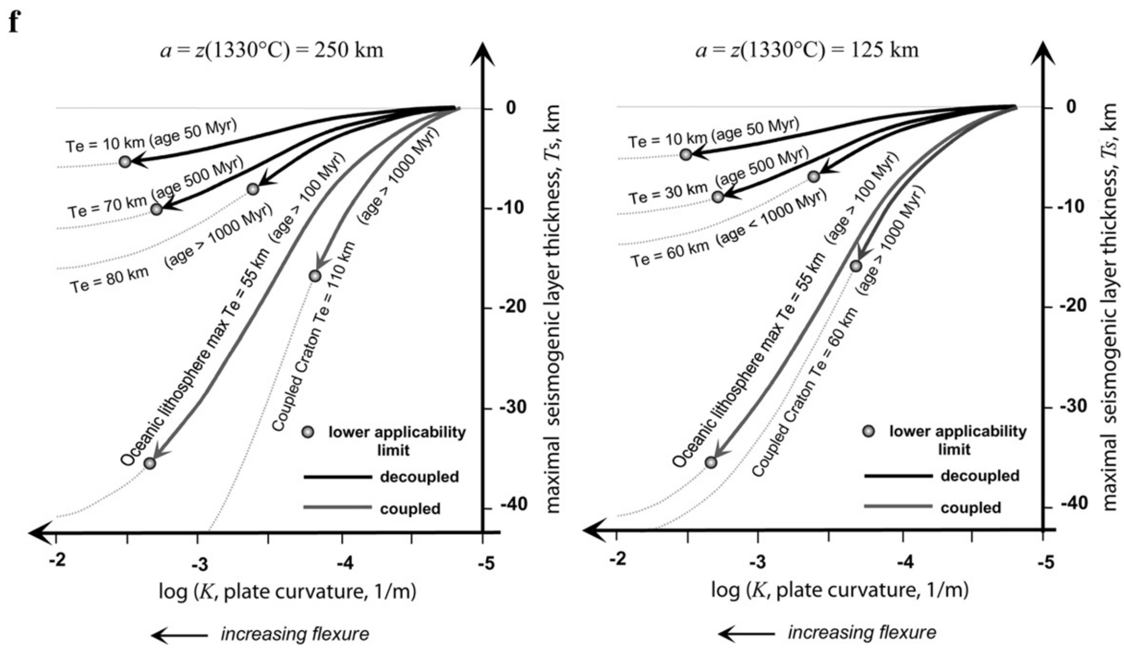

Fig. 7 (*continued*).

the same amount of flexure, compared to a single plate. Consequently, T_e, which is a measure of integrated bending stress, is also reduced. T_e of a multilayer plate reflects the combined strength of all the brittle, elastic and ductile layers. Yet, it is not simply a sum of the thickness of these layers (h_1, h_2..., h_i..., h_n). Indeed, for a horizontally homogeneous multilayer elastic plate of thickness h composed of n layers with n neutral fibers z_{mi} ($z_{mi}=h_i/2$ in case of elastic plate; $h=\sum_{i=1}^{n} h_i$), the flexural moment and flexural rigidity are:

$$M(K)=\frac{E}{K(1-\nu^2)}\sum_{i=1}^{n}\int_{z_{h_i}^-}^{z_{h_i}^+}(z-z_{mi})^2dz$$

$$D=\frac{E}{(1-\nu^2)}\sum_{i=1}^{n}\int_{z_{h_i}^-}^{z_{h_i}^+}(z-z_{mi})^2dz=\frac{E}{12(1-\nu^2)}\sum_{i=1}^{n}h_i^3 \tag{4a}$$

where z_i^+ and z_i^- refer to the lower and upper interface of the ith layer so that $h_i=z_i^+-z_i^-$. Consequently, from the Eqs. (2a) and (4a) we get:

$$\frac{ET_e^3}{12(1-\nu^2)}=\frac{E}{12(1-\nu^2)}\sum_{i=1}^{n}h_i^3 \Rightarrow T_e(YSE)=\sqrt[3]{\sum_{i=1}^{n}h_i^3} \tag{4b}$$

In case of a visco-elasto-plastic plate (Eq. (2a)), z_{mi} and h_i and hence D are functions of K, and inelastic stresses should be also included in the integrals (4a) (see Burov and Diament, 1995 for exact expressions). The contribution from the inelastic stresses can be also roughly accounted by adjusting the values of z_{mi} and h_i as functions of K, making the Eq. (4b) applicable to all stratified plates (provided that thin plate approximation is valid). In case of two equally strong layers ($n=2$) of total thickness h (e.g., crust and mantle), $T_e\approx0.6h$ instead of h, i.e. the integrated strength is reduced by a factor of 2 compared to a mono-layer plate (e.g. old craton with strong coupled lower crust). The meaning of T_e (*YSE*) in the continents thus becomes clearer. It reflects the integrated effect of *all* competent layers that are involved in the support of a load, including the weak ones. Fig. 7a shows prediction of T_e in the unflexed continental lithosphere, as a function of age and crustal thickness (compared to the oceanic lithosphere, crustal thickness appears as important as thermal age in defining the integrated strength of the continental lithosphere).

If the multi-layered continental lithosphere is subject to large loads, it flexes, and the curvature of the deformed plate, K, increases. T_e (*YSE*) is a function of K and is given (Burov and Diament, 1995, 1996) by (Fig. 7b,c):

$$T_e(YSE)=T_e(elastic)C(K,t,h_{c1},h_{c2}...), \tag{5}$$

where C is a function of the curvature, K, the thermal age, t, and the rheological structure. A precise analytical expression for C is bulky (Burov and Diament, 1992), although Burov and Diament (1996) provide a first-order approximation for a "typical" case of continental lithosphere with a mean crustal thickness of 35 km, a quartz-dominated crust, and an olivine dominated mantle, which, they indicate, is valid for $10^{-9}<K<10^{-6}\,\mathrm{m}^{-1}$. T_e (*YSE*) then simplifies to:

$$T_e(YSE)\approx T_e(elastic)\left(1-(1-K/K_{max})^{1/2}\right)^{(1/2+1/4(T_e(elastic)/T_e\,max))} \tag{6}$$

where K_{max} (in m^{-1})$=(180\times10^3(1+1.3T_e(\min)/T_e(\mathrm{elastic}))^6)^{-1}$, T_e (max) = 120 km, T_e (min) = 15 km, and T_e (elastic) is the initial elastic thickness prior to flexure, which can be evaluated from Eqs. (4a) and (4b).

We show in Fig. 7d–f, therefore, how T_e and T_s would be expected to change using the precise analytical formulations of Burov and Diament (1992, 1995). The figure illustrates how the thickness of the brittle and ductile layers evolve with different loads and, hence, curvatures. On bending, brittle failure and, hence, the potential for seismicity preferentially develops in the uppermost part of the crust. The onset of brittle failure in the mantle is delayed, however, and does not occur until the amount of flexure and, hence, curvature is very large. Observations of curvature in the regions of large continental loads provide constraints on the brittle strength of continental lithosphere. Curvatures range from $10^{-8}\,\mathrm{m}^{-1}$ for the sub-Andean to $5\times10^{-7}\,\mathrm{m}^{-1}$ for the West Taiwan foreland basins (Watts and Burov, 2003 and references therein). The highest curvatures are those reported by Kruse and Royden (1994) of $4–5\times10^{-6}\,\mathrm{m}^{-1}$ for the Apennine and Dinaride foreland. Fig. 7d,e shows, however, that plate curvatures of $10^{-6}\,\mathrm{m}^{-1}$ may not be sufficiently large to cause brittle failure in the sub-crustal mantle, *unless* the flexed plate is subject to an externally applied tectonic stress. In the case illustrated in Fig. 7, the stress required to cause failure in the sub-crustal mantle for this plate curvature is 350 MPa assuming "dry" Byerlee's law. This is already close to the maximum likely value for tectonic boundary loads (e.g., Bott, 1993), suggesting that brittle failure, and, hence, earthquakes in the mantle will be rare. Instead, seismicity will be limited to the uppermost part of the crust where rocks fail by brittle deformation, irrespective of the stress level. This limit does not apply, of course, to T_e. For curvatures up to $10^{-6}\,\mathrm{m}^{-1}$, Fig. 7 shows that continental T_e is practically always larger than T_s. Only for the highest curvatures (i.e. $K>10^{-6}\,\mathrm{m}^{-1}$) will $T_e<T_s$ and, interestingly, will the case that $T_s>T_e$ arise. Of course, stress estimates shown in Fig. 7b,d or e depend on the assumed rheology. In particular, frictional strength at depth may be several times smaller than the prediction of the Byerlee's law in case of pore fluid pressure (reduction by a factor of 5). Yet the presence of fluids will also reduce the ductile rock strength by same or higher amount. As a result the rock may choose to flow rather than to break; T_e will be reduced and plate curvature would be higher for the same load. It thus appears difficult to favour mantle "seismicity" by simple brittle strength reduction due to the presence of fluids.

Finally, it should be noted that the dependence of T_e and T_s on the state of stress and plate curvature may result in strong lateral variations of T_e and T_s both at local and regional scale. The computations (Burov and Diament, 1995) demonstrate that surface loads (elevated topography or sedimentary loading; plate boundary forces) may result in strong lateral variations of both T_e and T_s. Surface or subsurface loading may decrease T_e (and increase T_s) by 30%–50% (or more in case of initially weak plates). In particular, the lithosphere beneath mountain ranges or large sedimentary basins (rifts, forelands) may be significantly weakened resulting in more "local" compensation of the surface loads. In subduction/collision zones, localized weakening due to plate bending under boundary forces may result in steeper slab dip and accelerated slab break-off. In case of weakened lithosphere (e.g., abnormal heat flux), loading may result in total failure of the plate (= local isostasy).

5. Intraplate seismicity (T_s), T_e and the brittle–ductile transition

Intra-plate seismicity is concentrated in a layer whose thickness (15–20 km in average) rarely exceeds 40–50 km both in oceanic and continental lithosphere, although deep mantle earthquakes are also well detected (e.g., Deverchere et al. 1991; Monsalve et al., 2006). Brittle properties of the oceanic and continental lithosphere are not expected to be different, it is thus natural to suppose that the similarity of T_s in oceans and adjacent continents is suggestive of the tectonic stress transition from oceanic to continental domain.

The mechanical considerations suggest that T_s has its own significance. It was previously concluded (e.g., Cloetingh and Wortel, 1986; Molnar and Lyon-Caen, 1988; Zoback, 1992; Bott, 1993) that: (1) average tectonic stresses do not exceed 100–600 MPa, and intra-plate forces – 10^{13} Nm; (2) brittle strength linearly increases with the confining pressure (Byerlee's law) because it defines the level of normal stress on the potential or active fault surfaces (σ_n in Eq. (2b)). The confining pressure, $\sigma^d_{ii}+\rho gz$, is almost a linear function of depth, z. σ^d_{ii} is non-lithostatic pressure due to deformation that does not exceed few hundred MPa; Byerlee's law thus predicts practically linear dependence of brittle strength with depth (Figs. 1b and 7b). Near the surface, brittle strength is 0–20 MPa while it is 100 times higher (2GPa) in the mantle. Figs. 4 and 7b,d,e demonstrate that bending stress, and thus the probability to reach brittle strength limits, decreases while approaching the neutral surface. Consequently, for any or both of the above two reasons (1–2), the upper crustal layers should fail easier than the lower mantle layers. At 50 km depth, which is the maximal observed depth of distributed seismicity, brittle rock strength in continents is 2 GPa (Fig. 7d,e). Assuming 100 km thick lithosphere, one needs a horizontal tectonic force of 10^{14} Nm to exceed this strength. The magnitude of this critical force is one or two orders of magnitude higher than the estimates for intra-plate forces. The 2 GPa stress level thus may probably be reached only locally, when one combines tectonic stresses with bending stresses. One can also argue that Byerlee's law is not valid for depths in excess of 40–50 km. One can expect that for such depths a different, lower stress aseismic plastic deformation mechanism (i.e., Pierls plasticity) can be easier activated than Byerlee's failure (see discussion in Burov, 2007).

As mentioned above, the discussions on rheology arrive not only from uncertainties of the rheology laws but also from the conflicting results on T_e from a number of continental studies. But, it is widely agreed that oceanic T_e data are robust. Hence, through understanding T_e–T_s relations for oceans we can progress with their understanding for continents. When all oceanic T_s data and T_e data are plotted on the same depth plot, there is an impression of correlation between T_s and T_e (Fig. 5). Yet when one separates the extensional and compressional events, the correlation breaks down (Fig. 5): detectable extensional earthquakes are systematically found at two times smaller depth than the corresponding T_e values (Watts and Burov, 2003). Indeed, the Byerlee's law predicts that extensional failure requires nearly two times smaller stress, which leads to conclusion that the earthquake depths are controlled by intra-plate stress level, and decrease with increasing integrated strength of the lithosphere B if $B>F$ (for a fixed F):

$$T_s \approx \Upsilon\left(F/T_e + \sigma^f_{xx}|_{z=T_s}\right)/\rho g$$
$$T_e(\text{oceans}) <\approx 0.7 h_m \qquad (7)$$

The factor $\Upsilon = 0.6^{-1}$–0.85^{-1} (Burov, 2007), $\sigma^f_{xx}|_{z=Ts}$ is flexural stress (by unit length (m) in out-of plane directon) at depth $z=T_s$. Eq. (7) shows that T_s decreases with increasing T_e. Thus T_s and T_e do not correlate but anti-correlate if $F<B$ (i.e., if plate preserves integrity, e.g. in subduction settings). For unbent plate, T_s can be equal to T_e only if $T_e = (0.8F/\rho g)^{1/2}$ (as the force, the denominator is also by unit length (m) in

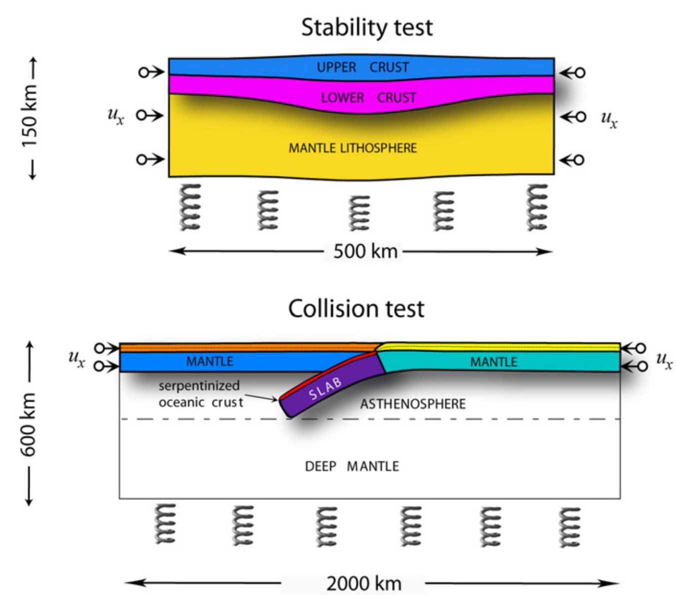

Fig. 8. Numerical model set-up. Springs indicated below each model symbolise hydrostatic boundary condition at the bottom. The upper surface is free. a) The stability test is based on a mountain range of height 3 km and width 200 km that is initially in isostatic equilibrium with a 36 km thick crust. We disturbed the isostatic balance by applying a horizontal compression to the edges of the lithosphere at a rate of 5 mm yr^{-1}. The displacements of both the surface topography and Moho were then tracked through time. b) The collision test was based on a continent/continent collision that was initiated by subduction of a dense, downgoing, oceanic plate. We assumed a normal thickness continental and oceanic cru t (36 and 7 km, respectively), a total convergence rate of 60 mm yr^{-1}, and a serpentinized subducted oceanic crust (Rupke et al., 2002). Rheological properties and other parameters are as given in Table 1.

out-of plane direction). Since $F<10^{13}$ Nm (by unit length) this implies $T_s<15$–16 km, whereas T_e of the plate shown in Fig. 4 is 30 km, i.e. $\approx 2\,T_s$. For smaller F, $T_s<1/2T_e$. Flexural stress σ^{f}_{xx} may increase the value of T_s by a factor of 2–3, but at the same time it would decrease T_e by the same factor (Fig. 4). Thus the two values, T_s and T_e, do not approach each other until the plate preserves its integrity ($F<B$). Maximal intra-plate stress

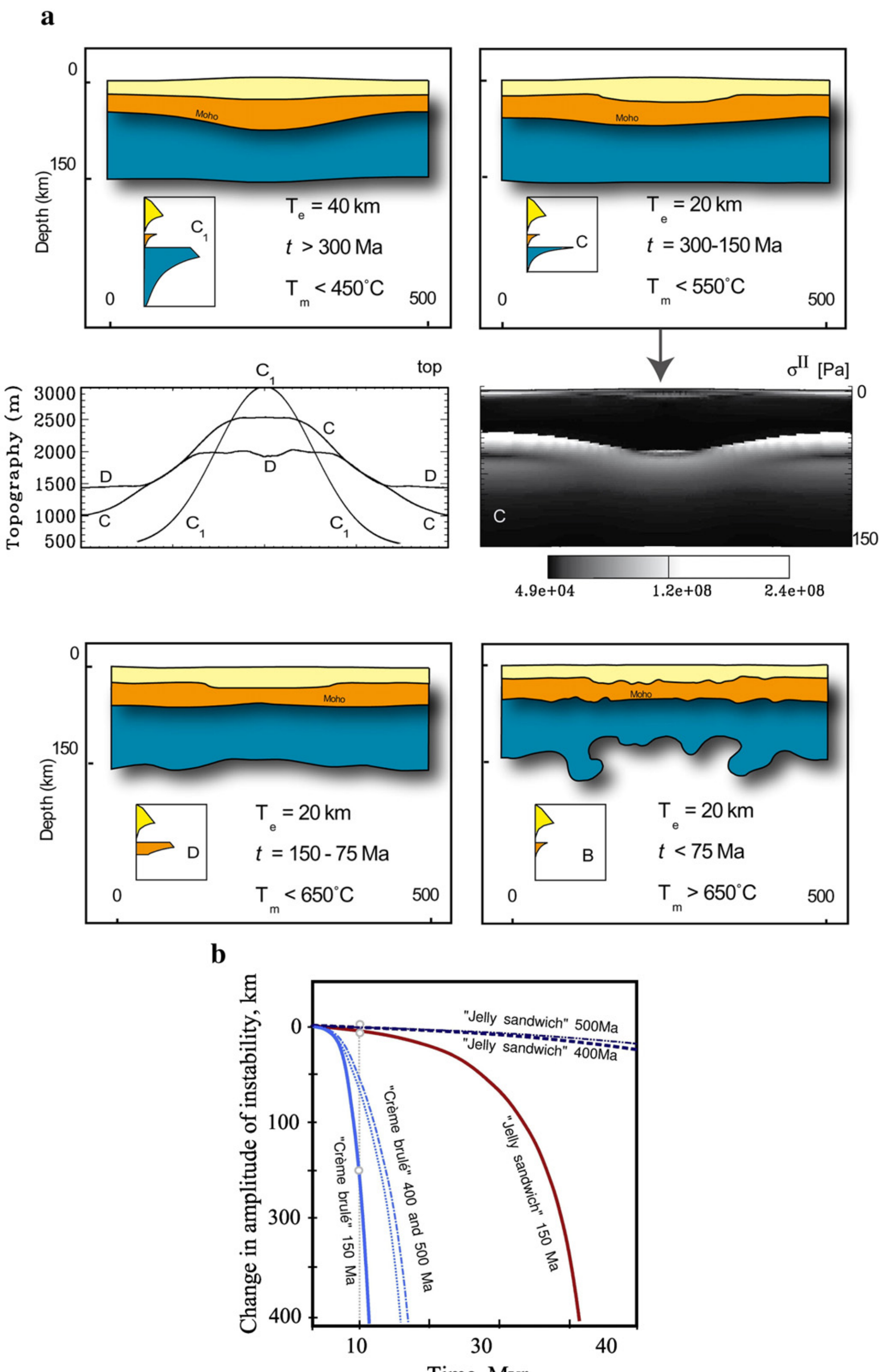

Fig. 9. a. Thermo-mechanical numerical tests of the stability of a mountain range using the failure envelopes associated with the jelly sandwich (Fig. 3d, or Fig. 5b of Jackson (2002)) and crème-brûlée (Fig. 3b, d or Fig. 5d of Jackson (2002) rheology models. The thermal structure is equivalent to that of a 150 Myr-old plate. Crustal and mantle structure after 10 Myr has elapsed. Middle of the figure shows surface topography evolution for rheologies C1, C (jelly sandwich) and D (crème brulée), left, and effective shear stress distribution for the case C. Note rapid topography collapse in case D whereas cases C1 and C are stable. After Burov and Watts (2006). b. The amplitude of the mantle root instability as a function of time. The figure shows the evolution of a marker that was initially positioned at the base of the mechanical lithosphere (i.e. the depth where the strength = 10 MPa). This initial position is assumed to be at 0 km on the vertical plot axis. The solid and dashed lines show the instability for a weak, young (thermo-tectonic age = 150 Myr) and strong, old (thermo-tectonic age = 400 or 500 Myr-old) plate respectively. After Burov and Watts (2006).

($\sigma^{f}_{xx}+F/T_e$) is theoretically limited to 2 GPa (upper bound). This yields T_s<40–50 km (for T_e<110 km), which is compatible with the observations (Maggi et al., 2000).

As seen from Fig. 4, strong mechanical core associated with T_e is centred at the neutral plane of the plate, z_n, whereas the seismogenic layer T_s is shifted to the surface. This is the reason why T_s cannot have same geometric interpretation as T_e. Since bending stresses are minimal near z_n, the earthquakes will be favoured at some vertical distance above or below it (Fig. 4a). The brittle strength linearly increases with depth, thus the earthquakes must be more frequent above z_n. For an elastic plate or brittle-elasto-ductile plate, z_n is located roughly in its middle (Fig. 4a), at a depth $z\approx1/2T_e(\max)$. In this case $T_s<1/2T_e$. If plate strength is concentrated in the brittle-elastic layer T_s then earthquakes would occur at depths $\leq(T_e(\max)-T_e)$, Fig. 7f. On the other hand, $T_e(\max)-T_e<1/2T_e$ except for improbably strong flexure. Hence, in a brittle-elastic plate, the equity $T_s=T_e$ is impossible, as already mentioned above in the discussion on Fig. 4. T_s may be equal to T_e only in a plate with approximately *symmetric* strength distribution, i.e. in a plate comprising *equally* strong brittle and ductile part (Fig. 4a), which is incompatible with crème-brûlée rheology model (Fig. 4b).

Rock mechanics data suggest that in addition to Byerlee's law, a semi-brittle/semi-ductile strain rate dependent plastic flow may increasingly occur starting from 10–15 km depth, with a frictional component that is no longer significant at depths >40–50 km (Ranalli, 1995; Chester, 1995; Bos and Spiers, 2002). This also explains why intra-plate seismicity both in the oceanic and continental lithosphere is limited to 40–50 km depth.

There are, of course, regions where earthquakes extend to great depths (>40–50 km), for example, in subduction–collision zones, including continents (Monsalve et al., 2006). It is generally agreed (Scholz, 1990; Kirby et al., 1991) that this seismicity is not related to frictional sliding, at least not the Byerlee's law, but to some other metastable mechanisms. These mechanisms are only weakly related to rock strength. For example, it has been known for some time that, unlike shallow (i.e. depths <50–70 km) earthquakes, deep earthquakes produce very few aftershocks. This aftershock behaviour is a strong argument that the earthquake generating mechanism differs between shallow and deep earthquakes. The physical mechanisms of deep (>30–40 km) earthquakes are still to be understood but it is agreed that the differential stresses needed to initiate these earthquakes are smaller that the predictions of the Byerlee's law for dry rock at corresponding depth but are greater than that for shallow earthquakes (15–25 km depth) (Kirby et al., 1991).

6. Simple physical considerations

In crème-brûlée models, lithospheric mantle is mechanically indistinguishable from the asthenosphere. This implies very low effective viscosities of 10^{19}–10^{20} Pa s. Here we explore whether low-viscosity mantle lithosphere is highly unstable to sinking convectively. Does the persistence of mantle lithosphere require high strength, or does it allow the possibility of such low viscosities?

The mean heat flow in Archean shield regions is ~40 mW m^{-2}, which increases to ~60 mW m^{-2} in flanking orogenic belts (Jaupart and Mareschal, 1999). As Pinet et al. (1991) have shown, a significant part of

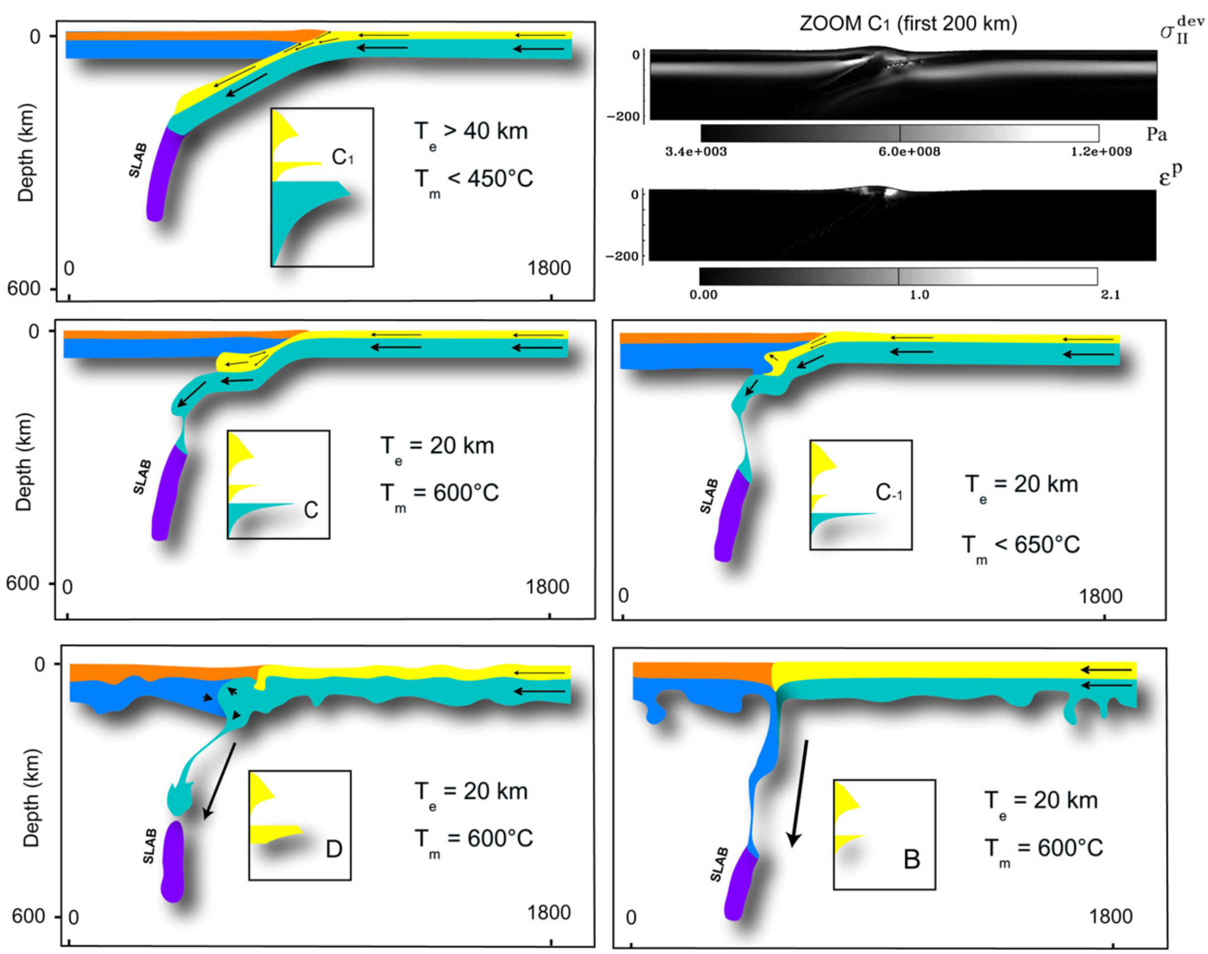

Fig. 10. Numerical tests of the stability of a continental collisional system using various possible failure envelopes (Fig. 1a). The figure shows a snapshot at 5 Myr of the structural styles that develop after 300 km of shortening. Insert to right of case C$_1$ shows zoom of first 200 km in depth, with the effective shear stress (top) and plastic brittle strain (bottom). Note that despite high mantle strength, no brittle (seismic) deformation occurs below Moho depth except subduction channel.

this heat flow is derived from radiogenic sources in the crust. Therefore, temperatures at the Moho are relatively low (~400–600 °C). The mantle must therefore maintain a fixed, relatively high, viscosity which prevents convective heat advection to the Moho. Otherwise, surface heat flow would increase to >150 mW m^{-2} which would be the case in an actively extending rift (e.g. Sclater et al., 1980). Since heat flow this high is not observed in shields and orogens, then a thick, cool, stable mantle layer should remain that prevents direct contact between the crustal part of the lithosphere and the convective upper mantle.

The negative buoyancy of the mantle lithosphere at subduction zones is considered as a major driving force in plate tectonics. The evidence that the continental mantle is ~20 kg m^{-3} denser than the underlying asthenosphere and is gravitationally unstable has been reviewed by Stacey (1992), among others. Although this density contrast is commonly accepted for Phanerozoic lithosphere, it is still a subject of debate whether it applies to the presumably Mg-rich and depleted cratonic lithospheres. Irrespective, volumetric seismic velocities, which are generally considered a proxy for density, are systematically higher in the lithosphere mantle than in the asthenosphere. Depending on its viscosity the mantle lithosphere therefore has the potential to sink as the result of a Rayleigh–Taylor (RT) instability (e.g., Houseman et al., 1981; Burov and Molnar, 2008).

We can estimate the instability growth time (i.e. the time it takes for a mantle root to be amplified by e times its initial value) using Chandrasekhar's (1961) formulation. In this formulation a mantle Newtonian fluid layer of viscosity, η, density, ρ_m, and thickness, d, is

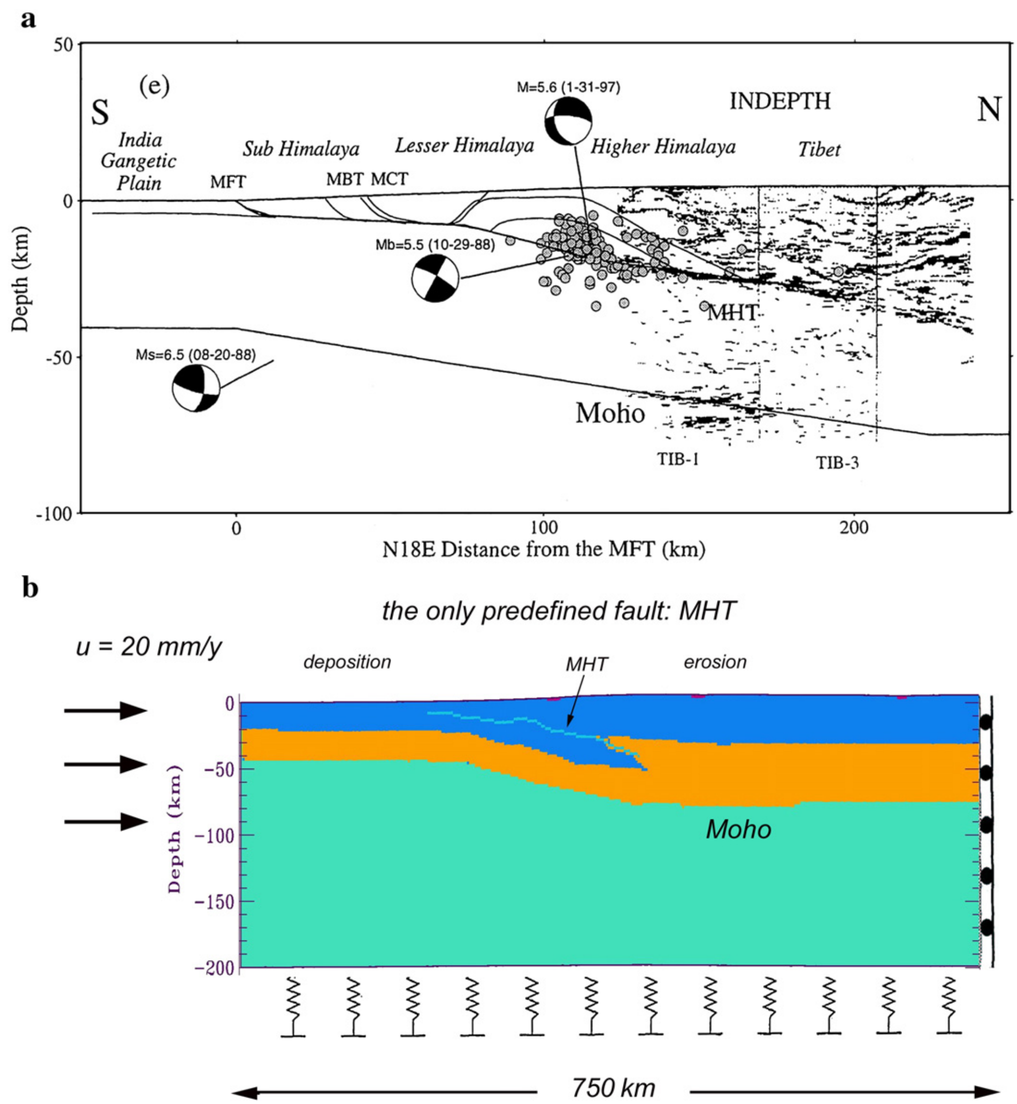

Fig. 11. a. Seismic data profile N18E (Cattin et al., 2001) through Himalaya that is used to construct the stability test of thermo-mechanical models shown below. Note that some seismic events are localized below the Moho depth (the data contested by Maggi et al. (2000) but re-confirmed by later studies (e.g., Monsalve et al., 2006). b. Setup of the numerical model based on enlarged N18E cross-section from (Cattin et al., 2001; panel a) and the general problem statement from (Toussaint et al., 2004b). Only one fault, the Major Himalayan Thrust (MHT) is pre-defined in the model as a pre-existing weak zone, by assuming zero cohesion for brittle rheology and by dripping the effective viscosity of the ductile rheology by a factor of 10). All other faults are expected to form automatically if the initial rheological assumptions are consistent. Visco-elasto-plastic rheology with Mohr-Coulomb plasticity and power-law non-linear viscosity (Table 1). Thermo-tectonic age of the Indian lithosphere — 700 Ma. Thermo-tectonic age of Tibetan lithosphere: 150 Ma. Convergence rate is 20 mm/yr. Color code: blue — upper crust; yellow — lower crust; green–blue — mantle. Surface erosion coefficient: 3000 m^2/yr according to (Toussaint et al, 2004b). c. Tests with JS rheology assuming dry diabase in the lower crust (insert on the right). Shown are material phase field (see panel b), strain rate field with faults that formed without being-predefined, and which geometry conforms the actually observed ones (panel a). Accumulated plastic (brittle) strain field at 3 Myr after onset of the experiment shows stably functioning brittle shear zones (faults) which depths and geometry are compatible with the observations (panel a). Maximal depths of brittle deformation (= maximal seismic depth), T_s, is 70 km, with some rare brittle strain accumulation zones in the mantle. d. Tests with CB rheology. See panels b and c for notations. Already at 2 Myr after onset of the experiment, the mantle becomes unstable and the geometry of the collision zones becomes strongly unstable; crustal geometry of the Indian plate does not resemble the observations and the lithosphere mantle tends to decouple from the crust. The predicted geometry of the faults does not fit the observations; the maximal depths of brittle deformation (= maximal seismic depth, T_s, is 25 km, i.e. 2–3 times smaller than the observed one).

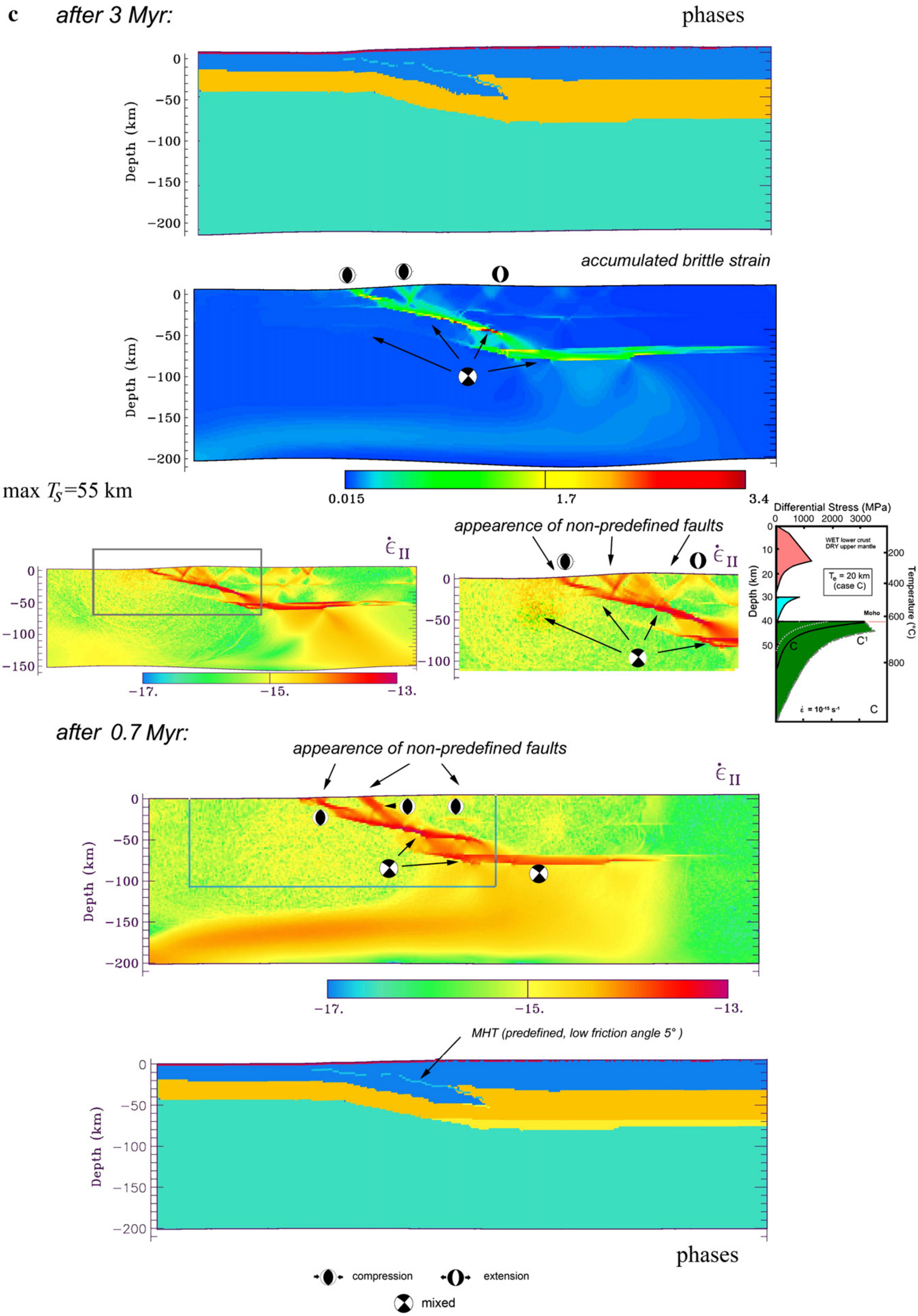

Fig. 11 (*continued*).

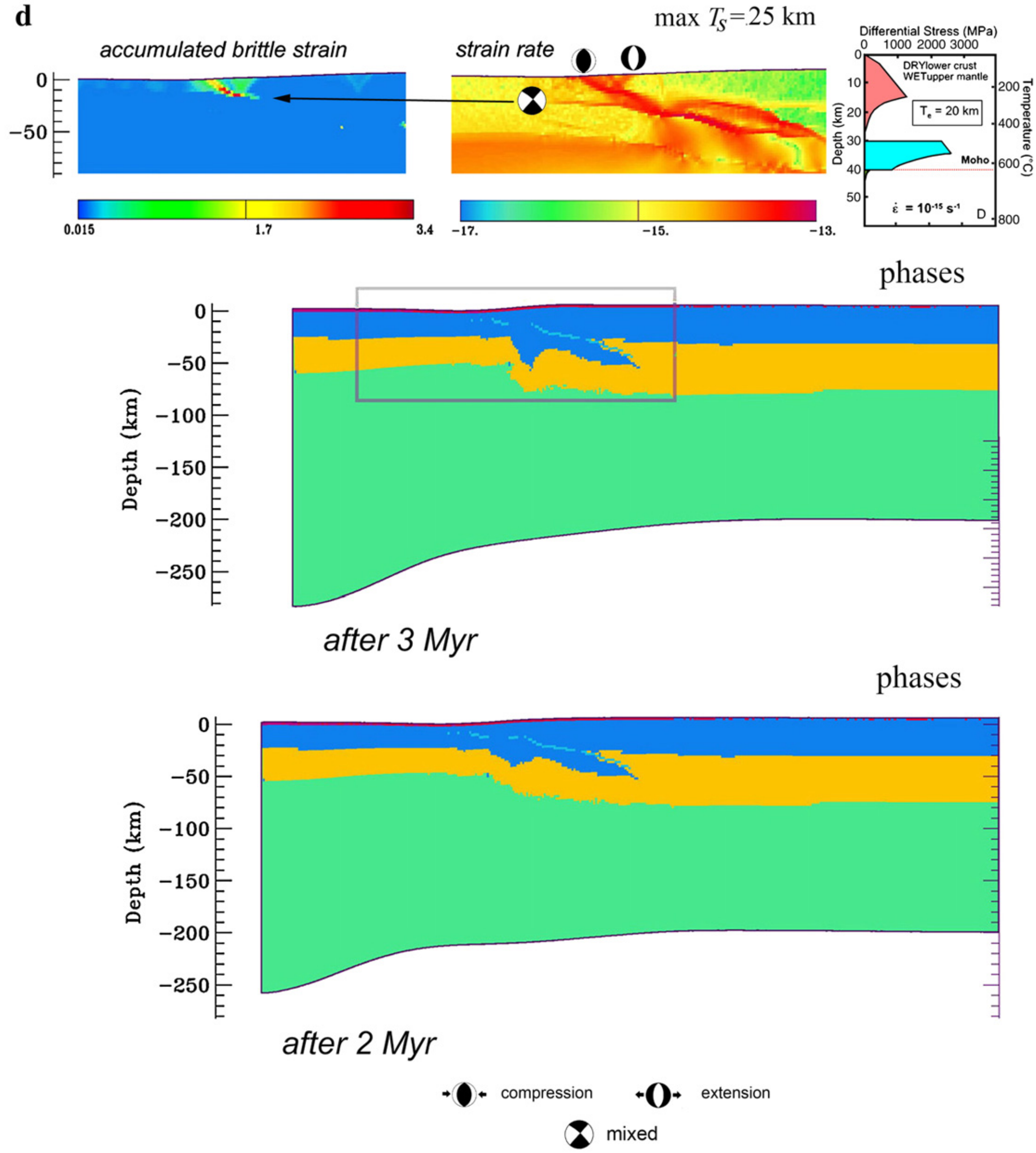

Fig. 11 (*continued*).

placed on top of a less dense fluid asthenospheric layer of density ρ_a and the same thickness. (We note that this formulation differs from that of Conrad and Molnar (1997) who used a fluid layer that is placed on top of a viscous half-space. However, both formulations are valid for instability amplitudes $<d$). The most rapidly growing instability wavelength, λ, is Ad where $2.5<A<3.0$ and the corresponding growth time, $t_{\min}$, is $B\eta((\rho_m-\rho_a)gd)^{-1}$ where $6.2.<B<13.0$ and g is average gravity. We can evaluate $t_{\min}$ for a particular η by assuming $(\rho_m-\rho_a)=20$ kg m^{-3} and $80<d<100$ km. If the continental mantle can support large stresses (>1–2 GPa) and has a high viscosity (10^{22}–10^{24} Pa s), as the jelly sandwich model implies, then $t_{\min}$ will be long (>100 Myr–2 Gyr). If, on the other hand, the stresses are small (0–10 MPa) and the viscosity is low (10^{19}–10^{20} Pa s), as the crème-brûlée model implies, then it will be short (0.1 Myr–2.0 Myr). This estimate predicts that a lithospheric mantle root would sink and possibly detach quickly in a crème brûlée model, and the corresponding surface mountains would dissipate so that no orogen would survive for more than a couple of Myr.

We have considered so far a Newtonian viscosity and a large viscosity contrast between the lithosphere and asthenosphere. However, a temperature dependent viscosity and power law rheology result in even shorter growth times than the ones derived here for constant viscosity (Conrad and Molnar, 1997; Molnar and Houseman, 2004). Furthermore, if either the viscosity contrast is small or the mantle root starts to detach, then Eqs. (1a) and (1b) in Weinberg and Podladchikov (1995) suggests that the entire system will begin to collapse at a vertical Stokes flow velocity of ~1 mm yr^{-1} for the jelly-sandwich model and ~100–1000 mm yr^{-1} for the crème-brûlée model. (We note that these flow velocities strongly depend on the sphere diameter which we assume to be λ). Therefore, using our assumption for the crème-brûlée model, surface topography would disappear in less than 0.02–2 Myr whereas it could be supported for as long as 100 Myr–2 Gyr for a jelly sandwich model.

7. Dynamic numerical models

In order to substantiate the growth times derived from simple viscous models, we carried out sensitivity tests using a large-strain numerical thermo-mechanical code (Flamar–Parovoz v12) that allows the equations of mechanical equilibrium for a visco-elasto-plastic plate, coupled with heat transfer equations, to be solved for *any* prescribed rheological strength profile (Poliakov et al., 1993). Similar models have been used by Toussaint et al. (2004a,b), for example, to determine the role that the geotherm, lower crustal composition, and metamorphic changes in the subducting crust may play on the evolution of continental collision zones. We ran two separate tests (Fig. 8) using rheological properties that matched the envelopes in Fig. 5B and D of Jackson (2002). Our aim of using these envelopes, which otherwise have a similar T_e, was to determine what the crème-brûlée and jelly sandwich models imply about the stability of mountain ranges and the structural styles that develop.

Fig. 9 shows the results of the stability tests. The figure shows a "snapshot" of the deformation after 10 Myr. We found that in the crème-brûlée model the crust and mantle already becomes unstable after 1.5–2.0 Myr. By 10 Myr, the lithosphere disintegrates due to delamination of the mantle followed by its convective removal and replacement with hot asthenosphere. This leads eventually to a flattening of the Moho and 'tectonic erosion' of the crustal root that initially supported the topography. The jelly sandwich model, on the other hand, is more stable and we found few signs of crust and mantle instability for the duration of the model run (10 Myr).

Fig. 10 shows the results of a collision test. The figure shows a "snapshot" of the deformation after 300 km of shortening which at 60 mm yr^{-1} takes 5 Myr. The jelly sandwich model is stable and subduction occurs by the underthrusting of a continental slab that, with or without the crust, maintains its overall shape. The crème-brûlée model, on the other hand, is unstable. There is no subduction and convergence is taken up in the 'suture' zone that separates the two plates. The crème-brûlée model is therefore unable to explain those features of collisional systems that require subduction such as kyanite and sillimanite grade metamorphism. The jelly sandwich model, on the other hand, can explain not only the metamorphism, but also some of the gross structural styles of collisional systems such as those associated with 'slab flattening' (e.g. Western North America; Humphreys et al., 2003), 'crustal doubling' (e.g. Alps — Giese et al., 1982), and 'arc subduction' (e.g. southern Tibet — Boutelier et al., 2003).

The final set of experiments (Fig. 11) shows the results of short-term collision tests applied to the present day geometry of the India–Tibet collision zone derived from seismic and gravity data (Cattin et al., 2001). In these experiments we used the same modelling techniques as for the experiments of the previous section, and many elements of the numerical problem setup are borrowed from our previous models of India–Himalaya "like" collision (Toussaint et al., 2004b). The main idea of these experiments was to test the stability of the present-day configuration of this collision zone, that has been stably acting since the last 50 Myr, for the next 1–3 Myr. We expect that if the rheological assumptions used for the model are valid, no dramatic modifications in the overall geometry should occur within this period of time, since the characteristic length-scale of main restructuring intervals in the history of the India–Himalaya collision zone was significantly larger than few Myr (e.g., Toussaint et al., 2004b). Also, we do not introduce any pre-existing brittle weakness zones in the model, except the major thrust fault MHT (Main Himalayan Thrust, introduced as a zero cohesion zone). This is done because it is expected that in the case of a "good" rheological choice, the predicted seismic and faulting patterns and depths should resemble the real observations. Three rheological assumptions have been tested: "standard" jelly-sandwich with quartz-diorite lower crust for Tibet and diabase crust for the Indian plate (Fig. 11c); crème-brulée (CB) with dry diabase lower crust and wet olivine mantle (Fig. 11d); jelly-sandwich (JS) with quartz–diorité lower crust for both plates (the results of this experiment are not shown as they resemble the results of the previous experiment of Fig. 11c). As can be seen, the presence of strong crust in "CB" case is not sufficient to keep the continental convergence stable, the mantle lithosphere is rapidly removed by the gravitational instabilities and convective movements in the asthenosphere, the crustal geometry does not resemble the observations even after 1–2 Myr; the faults have wrong geometries and the predicted seismicity zones are limited to shallow depths (~20–25 km). In case of jelly-sandwich rheology the collision not only stable during the entire duration of the experiments, but the geometry of the secondary activated fault zones resemble well the real geometries of the MFT, MBT, MCT (Main Frontal Thrust fault, Main Boundary Thrust, Main Central Thrust, respectively, see Fig. 11a), and the predicted maximal seismicity depths (up to 70 km) conform with the observations. This experiment confirms the analytical predictions of the previous sections that CB rheology is not compatible with deep seismicity: 50 km thick strong brittle crust would generate "flexural" seismicity only at 20–25 km depth. This is explained by the fact that in the absence of mechanical coupling with strong mantle lithosphere layer, the lowermost part of the down-flexed crust undergoes differential compression that increases confining pressure and thus the brittle strength of the crust. Consequently, seismic events below the neutral fiber of the crust become impossible.

8. Discussion and conclusions

We have shown here that the observations of flexure and the results of thermal and mechanical modelling are compatible with the view that mantle part of the lithosphere is strong and is capable of supporting stresses (and geological loads) for long periods of time. T_e values derived from forward flexural models as well as from adequately formulated (in terms of the mechanical problem) inverse models provide sufficiently robust constraints on the integral long-term strength of the lithosphere.

The suggested method of testing rheology by direct thermo-mechanical modelling can be used for parameterization of laboratory-based rheology laws.

Eq. (7) demonstrates incompatibility between T_e and T_s for oceanic or mechanically coupled lithosphere. Small "T_s-like "continental T_e values obtained from FAA admittance continental studies (McKenzie and Fairhead, 1997; Jackson, 2002) and from some other flexural models most probably stem from inadequate formulation of the mechanical (flexural) problem in these models. When the flexural problem is formulated in mechanically correct way, i.e. accounts for all major topography loads are boundary forces and moments, both FAA and Bouguer anomaly based methods provide compatible T_e estimates that confirm previous T_e estimates for continents. These T_e estimates do not correlate with T_s values and in many cases largely exceed them. Whatever is the most appropriate rheology for the continental lithosphere, we conclude that low T_e based on the analysis of McKenzie and Fairhead (1997) and Jackson (2002), cannot be valid, at least due to the mechanically inconsistent formulation of the flexural problem. We conclude that these small T_e are artefacts of incorrectly formulated mechanical problem in McKenzie and Fairhead (1997) and Jackson (2002), rather than of inconsistencies of the inverse methods themselves.

Oceanic flexure studies show that T_e is high and that large loads such as oceanic islands and seamounts are largely supported by the mantle lithosphere. While the role of the mantle in the continents is more difficult to quantify, there is evidence from cratonic regions and both forward and inverse (i.e. spectral) gravity modelling that T_e is high and can locally significantly exceed the crustal thickness.

We find no difficulty in reconciling the results of seismogenic layer, T_s, and elastic thickness, T_e, studies. While both parameters are proxies for the mechanical state of the lithosphere they are not the same. T_s reflects the level of stress in the uppermost weak brittle layer that responds on historical time-scales to stresses by faulting and earthquakes. T_e, in contrast, reflects the integrated strength of the entire lithosphere that responds to long-term ($>10^5$ a) geological loads by flexure. In most cases compatible with plate bending, T_s is significantly (~50%) smaller than T_e (Eq. (7)).

Deep (>20–25 km depth) crustal and mantle seismicity is only possible in case of JS rheology. CB rheology is not compatible with seismic events deeper that 25 km as in this case T_e is less than 40–

50 km while T_s is ~0.5T_e. Deep (>20–25 km depth) crustal seismicity of flexural origin requires strong mantle layer that is mechanically coupled to the crust. In the absence of such layer, the lower part of the crust is found in differential compression that results in increase of non-lithostatic pressure below 20–25 km depth and thus of the brittle strength of the crust. As consequence, crust becomes aseismic below its neutral fiber, i.e. below 20–25 km depth. On the contrary, when a strong lower crustal layer is coupled to strong mantle lithosphere, the neutral fiber may be shifted down to 40–55 km depth allowing for crustal seismicity just down to the Moho depth (~40 km). Consequently, the presence of deep crustal seismicity is proxy to the presence of strong mantle lithosphere, which must be mechanically coupled with the strong crust in this case. Deep crustal seismicity, when observed, indicates regions where CB rheology is not applicable.

There is almost certainly no one type of strength profile that characterises all continental lithosphere. We have only tested few possible models in this paper. Nevertheless, they are representative and thus useful. They are based on the same failure envelopes that Jackson (2002) used to argue that the mantle is weak, not strong. Moreover, they allow us to speculate on the stability of other models. The crème-brûlée model of Jackson (2002) yields a T_e of 20 km that is at the *high* end of the usual seismogenic layer thickness. We have already shown that the crème-brûlée model is buoyantly unstable. Therefore, weaker crème-brûlée models (e.g. ones with a weaker upper crust and T_e<20 km) will be even more unstable. The jelly sandwich model of Jackson (2002) yields a T_e of 20 km that is at the *low* end of continental T_e estimates. We have already shown that this model is stable. Stronger jelly sandwich models (e.g. ones with a strong lower crust and T_e>20 km) will be even more stable. The wide range of continental T_e estimates suggest that while the crème-brûlée model may apply to some syn-rift basins, margins and young orogens (e.g. Basin and Range), the jelly sandwich model, and its stronger variants, is more widely applicable (intra-continental and old orogens, forelands, shields and post-rift basins).

Both in oceans and continents, the maximal depths of distributed seismicity are comparable (40–50 km), indicating that they are primarily limited by the level of the confining pressure, which linearly grows with depth and has similar values at 40–50 km depth both in the oceanic and continental plates. In oceans, 40 km depth is found in the mantle, in continents this depth coincides with the Moho boundary. This explains why continental seismicity primarily occurs in the crust. Moho is a rheological boundary; in case of JS rheology with crust–mantle decoupling, it forms a mechanically weak interface associated with non-lithostatic stress drop. Consequently, stress transmission from crust to mantle is attenuated explaining the rareness of seismicity in the mantle just below the Moho, while at larger depths brittle seismicity is prohibited by the increasing confining pressure. Mantle seismicity may happen when initially mechanically coupled crustal and mantle layers become locally uncoupled. This may happen, for example, due to strong downward flexure (Burov and Diament, 1995, Fig. 7d,e). In this case the uppermost mantle may be found in strong flexural tension; this leads to a local drop in the brittle strength of the mantle. Consequently, mantle may become locally seismic.

In case of strong crust–mantle coupling (coupled JS rheology), Moho depth appears to coincide with the neutral fiber (low stress zone) of the bending lithosphere, and seismicity below the Moho depth becomes nearly impossible. The practical absence of deep mantle seismicity is limited by insufficient stress levels compared to the growing brittle strength: in case of mechanically coupled strong crust and mantle this is actually the case because the neutral fiber, i.e., zone of minimal flexural stress, occurs near the Moho depth. In case of crust–mantle decoupling (JS rheology *senso stricto*), flexural stresses and flexure in the mantle should be improbably large (on the GPa level) to provoke brittle failure below 35–40 km depth. Both the geodynamic stress estimates and the observed curvatures of plate flexure (Fig. 7d–f) prohibit such stress levels.

Thermo-mechanical modelling of lithospheric deformation suggests that the persistence of topographic features and their compensating roots requires that the sub-crustal mantle is strong and able to act as both a stress guide and a support for surface loads. It might be thought that it would not matter which competent layer in the lithosphere is the strong one. However, our tests show that the density contrast between the crust and mantle is sufficient to ensure that it is the mantle, rather than the crust, which provides both the stress guide and support. In our view, subduction and orogenesis, *require* a strong mantle layer. We have found this to be true irrespective of the actual strength of the crust. Weak mantle is mechanically unstable and tends to delaminate from the overlying crust because it is unable to resist forces of tectonic origin. Once it does delaminate, hotter and lighter mantle asthenosphere can flow upward to the Moho. The resulting increase in Moho temperature would lead to extensive partial melting and magmatic activity as well as further weakening such that subduction is inhibited and surface topography collapses in a relatively short interval of time.

We conclude that rheological models such as crème-brûlée which invoke a weak lithosphere mantle are generally incompatible with observations. The jelly sandwich is in better agreement and we believe provides a useful first-order explanation for the long-term support of the Earth's main surface features.

Acknowledgements

Previous work with A.B. Watts has largely contributed to the development of this study. I also thank both anonymous reviewers for highly useful comments.

References

Barrell, J., 1914. The strength of the Earth's crust. I. Geologic tests of the limits of strength. J. Geol. 22, 28–48.
Byerlee, J.D., 1978. Friction of rocks. Pure Appl. Geophys. 116, 615–626.
Bos, B., Spiers, C.J., 2002. Frictional-viscous flow in phyllosilicate-bearing fault rock: microphysical model and Implications for crustal strength profiles. J. Geophys. Res. 107 (B2), 2028. doi:10.1029/2001JB000301.
Bott, M.H.P., 1993. Modelling the plate-driving mechanism. J. Geol. Soc. (Lond.) 150, 941–951.
Boutelier, D., Chemenda, A., Burg, J.-P., 2003. Subduction versus accretion of intra-oceanic volcanic arcs: insight from thermo-mechanical analogue experiments. Earth Planet. Sci. Lett. 212, 31–45.
Brace, W.F., Kohlstedt, D.L., 1980. Limits on lithospheric stress imposed by laboratory experiments. J. Geophys. Res. 85, 6248–6252.
Burov, E.B., Kogan, M.G., Lyon-Caen, H., Molnar, P., 1990. Gravity anomalies, the deep structure, and dynamic processes beneath the Tien Shan. Earth Planet. Sci. Lett. 96, 367–383.
Burov, E.B., Diament, M., 1992. Flexure of the continental lithosphere with multilayered rheology. Geophys. J. Int. 109, 449–468.
Burov, E.B., Diament, M., 1995. The effective elastic thickness (Te) of continental lithosphere: what does it really mean? J. Geophys. Res. 100, 3895–3904.
Burov, E.B., Diament, M., 1996. Isostasy, effective elastic thickness (EET), and inelastic rheology of continents and oceans. Geology 24 (5), 419–422.
Burov, E.B., Molnar, P., 1998. Gravity anomalies over the Ferghana Valley (central Asia) and intracontinental deformation. J. Geophys. Res. 103, 18,137–18,152.
Burov, E., Watts, A.B., 2006. The long-term strength of continental lithosphere: “jelly-sandwich” or “crème-brûlée”? GSA Today 16, 4–10.
Burov, E.B., Plate rheology and mechanics, Ed.: G. Schubert, Treatise on Geophysics, Volume 6 — Crust and Lithosphere Dynamics (Volume Edt. A.B. Watts), Elsevier, TOGP00102, ISBN:978-0-444-51928-3, p 99–152, 611 pp, 2007.
Burov, E.B., Molnar, P., 2008. Small and large-amplitude gravitational instability of an elastically compressible viscoelastic Maxwell solid overlying an inviscid incompressible fluid: dependence of growth rates on wave number and elastic constants at low Deborah numbers. Earth Planet. Sci. Lett. 275 (3–4), 370–381.
Burov, E.B., Mareschal, J.-C., Jaupart, C., 1998. Large scale crustal inhomogeneities and lithospheric strength in cratons. Earth Planet Sci. Lett. 164, 205–219.
Caporali, A., 1995. Gravity anomalies and the flexure of the lithosphere in the Karakoram, Pakistan. J. Geophys. Res. (ISSN: 0148-0227) 100 (b8), 15075–15085.
Caporali, A., 2000. Buckling of the lithosphere in Western Himalaya: constraints from gravity and topography data. J. Geophys. Res. (ISSN: 0148-0227) 105, 3103–3113.
Caristan, Y., 1982. The transition from high temperature creep to fracture in Maryland diabase. J. Geophys. Res. 87, 6781–6790.
Carter, N.L., Tsenn, M.C., 1987. Flow properties of continental lithosphere. Tectonophysics 136, 27–63.

Cattin, R., Martelet, G., Henry, P., Avouac, J.P., Diament, M., Shakya, T.R., 2001. Gravity anomalies, crustal structure and thermo-mechanical support of the Himalaya of Central Nepal. Geophys. J. Int. 147 (2), 381–392.
Chandrasekhar, S., 1961. Hydrodynamic and Hydromagnetic Stability. Oxford University Press, Oxford.
Chapin, D.A., 1996. The theory of the Bouguer gravity anomaly: a tutorial. Lead. Edge 361–363.
Chapman, Y., 1986. Thermal gradient in the continental crust. In: Dawson, J.B., et al. (Ed.), The Nature of the Continental Crust: Spec. Publ. Geol. Soc. London, vol. 24, pp. 63–70.
Chen, W.-P., Molnar, P., 1983. Focal depths of intracontinental and intraplate earthquakes and their implications for the thermal and mechanical properties of the lithosphere. J. Geophys. Res. 88, 4183–4214.
Chester, F.M., 1995. A rheologic model for wet crust applied to strike-slip faults. J. Geophys. Res. 100, 13,033–13,044.
Chopra, P.N., Paterson, M.S., 1984. The role of water in the deformation of dunite. J. Geophys. Res. 89, 7861–7876.
Cloetingh, S., Wortel, R., 1986. Stress in the Indo-Australian plate. Tectonophysics 132, 49–67.
Crosby, A.G., 2007. An assessment of the accuracy of admittance and coherence estimates using synthetic data. Geophys. J. Int. 171, 25–54.
Cochran, J.R., 1980. Some remarks on isostasy and the long-term behavior of the continental lithosphere. Earth Planet. Sci. Lett. 46, 766–2711.
Conrad, C.P., Molnar, P., 1997. The growth of Rayleigh–Taylor-type instabilities in the lithosphere for various rheological and density structures. Geophys. J. Int. 129, 95–112.
Deverchere, J., Houdry, F., Diament, M., Solonenko, N.V., Solonenko, A.V., 1991. Evidence for a seismogenic upper mantle and lower crust in the Baikal rift. Geophys. Res. Lett. 18 (6), 1099–1102.
Diament, M., Goslin, J., 1986. Emplacement of the Marion Dufresne, Lena and Ob seamounts (south Indian Ocean) from a study of isostasy. Tectonophysics 121, 253–262.
Ervin, C.P., 1977. Theory of the Bouguer anomaly. Geophysics 42, 1468.
Fairhead, J.D., Green, C.M., Blitzkow, D., 2003. The use of GPS in gravity surveys. Lead. Edge 954–959.
Forsyth, D.W., 1985. Subsurface loading and estimates of the flexural rigidity of continental lithosphere. J. Geophys. Res. 90, 12,623–12,632.
Giese, P., Nicolich, R., Reutter, K.-J., 1982. Explosion crustal seismic studies in the Alpine–Mediterranean region and their implications to tectonic processes. In: Berckhemer, H., Hsu, K.J. (Eds.), Alpine–Mediterranean Geodynamics. Am. Geophys. Union, pp. 347–376.
Gleason, G.C., Tullis, J., 1995. A flow law for dislocation creep of quartz aggregates determined with the molten salt cell. Tectonophysics 247, 1–23.
Goetze, C., Evans, B., 1979. Stress and temperature in the bending lithosphere as constrained by experimental rock mechanics. Geophys. J. R. Astron. Soc. 59, 463–478.
England, P., Richardson, S.W., 1980. Erosion and age dependence of continental heat flow. Geophys. J. Royal. Astr. Soc. 62, 421–437.
Hackney, R.I., Featherstone, W.E., 2003. Geodetic versus geophysical perspectives of the 'gravity anomaly'. Geophys. J. Int. 154, 35–43.
Handy, M.R., Brun, J.P., 2004. Seismicity, structure and strength of the continental lithosphere. Earth Planet. Sci. Lett. 223, 427–441.
Houseman, G.A., McKenzie, D.P., Molnar, P., 1981. Convective instability of a thickened boundary layer and its relevance for the thermal evolution of continental convergent belts. J. Geophys. Res. 86, 6135–6155.
Humphreys, E.D., Hessler, E., Dueker, K., Farmer, G.L., Erslov, E., Atwater, T., 2003. How Laramide-age hydration of North American lithosphere by the Farallon slab controlled subsequent activity. Int. Geol. Rev. 45, 575–595.
Jackson, J., 2002. Strength of the continental lithosphere: time to abandon the jelly sandwich? GSA Today September, 4–10.
Jaupart, C., Mareschal, J.C., 1999. The thermal structure and thickness of continental roots. Lithos 48, 93–114.
Jin, Y., McNutt, M.K., Zhu, Y., 1994. Evidence from gravity and topography data for folding in Tibet. Nature 371, 669–674.
Jordan, T.A., Watts, A.B., 2005. Gravity anomalies, flexure and the elastic thickness structure of the India–Eurasia collisional system. Earth Planet. Sci. Lett. 166 (3), 1015–1038.
Judge, Anne, McNutt, M.K., 1991. The relationship between plate dip and elastic plate thickness: a study of the Peru–Chile Trench. J. Geophys. Res. 96, 16,625–16,639.
Le Pichon, X., Francheteau, J., Bonnin, J., 1973. Plate Tectonics. Elsevier Scientific. 300 pp.
Li, X., Götze, H.-J., 2001. Tutorial; ellipsoid, geoid, gravity, geodesy, and geophysics. Geophysics 66, 1660–1668.
Lyon-Caen, H., Molnar, P., 1983. Constraints on the structure of the Himalaya from an analysis of gravity anomalies and a flexural model of the lithosphere. J. Geophys. Res. 88, 8171–8191.
Lyon-Caen, H., Molnar, P., 1984. Gravity anomalies and the structure of the western Tibet and the southern Tarim Basin. Geophys. Res. Lett. 11, 1251–1254.
Kirby S.H., and Kronenberg, Rheology of the lithosphere: selected topics, *Rev. Geophys.*, 25, 1219–1244 (a) and correction 1680–1681 (b), 1987a,b.
Kirby, S.H., Durham, W., Stern, L., 1991. Mantle phase changes and deep-earthquake faulting in subducting lithosphere. Science 252, 216–225.
Kruse, S., Royden, L., 1994. Bending and unbending of an elastic lithosphere: the Cenozoic history of the Apennine and Dinaride foredeep basins. Tectonics 13, 278–302.
Lafehr, T.R., 1991. Standardization in gravity reduction. Geophysics 56 (8), 1170–1178.
Lowry, A.R., Smith, R.B., 1994. Flexural rigidity of the Basin and Range–Colorado Plateau–Rocky Mountain transition from coherence analysis of gravity and topography. J. Geophys. Res. 99, 20,123–20,140.
Mackwell, S.J., Zimmerman, M.E., Kohlstedt, D.L., 1998. High-temperature deformation of dry diabase with applications to tectonics on Venus. J. Geophys. Res. 103, 975–984.
Maggi, A., Jackson, J.A., Priestley, K., Baker, C., 2000. A re-assessment of focal depth distributions in southern Iran, the Tien Shan and northern India: do earthquakes occur in the continental mantle? Geophys. J. Int. 143, 629–661.
McAdoo, D.C., Martin, C.F., Polouse, S., 1985. Seasat observations of flexure: evidence for a strong lithosphere. Tectonophysics 116, 209–222.
McKenzie, D.P., Fairhead, D., 1997. Estimates of the effective elastic thickness of the continental lithosphere from Bouguer and free-air gravity anomalies. J. Geophys. Res. 102, 27,523–27,552.
McNutt, M.K., Menard, H.W., 1982. Constraints on yield strength in the oceanic lithosphere derived from observations of flexure. Geophys. J. R. Astron. Soc. 71, 363–395.
Molnar, P., Houseman, G.A., 2004. The effects of bouyant crust on the gravitational instability of thickened mantle lithosphere at zones of intracontinental convergence. Geophys. J. Int. 158, 1134–1150.
Molnar, P., Lyon-Caen, H., 1988. Some simple physical aspects of the support, structure, and evolution of mountain belts. Geol. Soc. Am. Spec. Pap. 218, 179–207.
Monsalve, G., Sheehan, A., Schulte-Pelkum, V., Rajaure, S., Pandey, M.R., Wu, F., 2006. Seismicity and one-dimensional velocity structure of the Himalayan collision zone: earthquakes in the crust and upper mantle. J. Geophys. Res. 111. doi:10.1029/2005JB004062.
Naudy, H., Neumann, R., 1965. Sur la définition de l'anomalie de Bouguer et ses conséquences pratiques. Geophys. Prospect. 13, 1–11.
Parsons, B.E., Sclater, J.G., 1977. An analysis of the variation of ocean floor bathymetry and heat flow with age. J. Geophys. Res. 82, 803–827.
Patella, D., 1988. Tutorial: an unambiguous derivation of the Bouguer gravity anomaly. Boll. Geofis. Teor. Appl. XXX (119–120), 345–352.
Pérez-Gussinyé, M., Watts, A.B., 2005. The long-term strength of Europe and its implications for plate-forming processes. Nature 436. doi:10.1038/nature03854 21 July.
Pinet, C., Jaupart, C., Mareschal, J.-C., Gariepy, C., Bienfait, G., Lapointe, R., 1991. Heat flow and lithospheric structure of the eastern Canadian shield. J. Geophys. Res. 96, 19,923–19,941.
Poliakov, A.N.B., Cundall, P., Podladchikov, Y., Laykhovsky, V., 1993. An explicit inertial method for the simulation of visco-elastic flow: an evaluation of elastic effects on diapiric flow in two- or three-layers models. In: Stone, D.B., Runcorn, S.K. (Eds.), Flow and Creep in the Solar System: Observations, Modelling and Theory, Dynamic Modelling and Flow in the Earth and Planets Series, pp. 175–195.
Ranalli, G., 1995. Rheology of the Earth, 2nd ed. Chapman and Hall, London. 413 pp.
Rupke, L.H., Morgan, J.P., Hort, M., Connolly, J.A.D., 2002. Are the regional variations in Central American arc lavas due to differing basaltic versus peridotitic slab sources of fluids? Geology 30, 1035–1038.
Rutter, E.H., Brodie, K.H., 1991. Lithosphere rheology — a note of caution. J. Struct. Geol. 13, 363–367.
Scholz, C.H., 1990. Mechanics of faulting. Annu. Rev. Earth Planet. Sci. 17, 309–334.
Sclater, J.G., Jaupart, C., Galson, D., 1980. The heat flow through oceanic and continental crust and the heat loss of the Earth. J. Geophys. Res. 18, 269–311.
Shelton, G., Tullis, J.A., 1981. Experimental flow laws for crustal rocks. Trans. Am. Geophys. Union 62, 396.
Stacey, F.D., 1992. Physics of the Earth. Brookfield Press, Brisbane. 513 pp.
Timoshenko, S.P., Woinowsky-Krieger, S., 1959. Theory of Plates and Shells. McGraw-Hill, N.Y. 580 pp.
Toussaint, G., Burov, E., Jolivet, L., 2004a. Continental plate collision: unstable vs. stable slab dynamics. Geology 32, 33–36.
Toussaint, G., Burov, E., Avouac, J.-P., 2004b. Tectonic evolution of a continental collision zone: a thermo mechanical numerical model. Tectonics 23, TC6003. doi:10.1029/2003TC001604.
Turcotte, D.L., Schubert, G., 2002. Geodynamics, 2nd ed. Cambridge University Press. 456 pp.
Watts, A.B., 1978. An analysis of isostasy in the world's oceans: 1. Hawaiian–Emperor Seamount Chain. J. Geophys. Res. 83, 5,989–6,004.
Watts, A.B., 1992. The elastic thickness of the lithosphere and the evolution of sedimentary basins. Basin Res. 4, 169–178.
Watts, A.B., 2001. Isostasy and Flexure of the Lithosphere. Cambridge University Press, Cambridge. 458 pp.
Watts, A.B., Burov, E., 2003. Lithospheric strength and its relationship to the elastic and seismogenic layer thickness. Earth Planet Sci. Lett. 213, 113–131.
Weinberg, R.F., Podladchikov, Y., 1995. The rise of solid state diapirs. J. Struct. Geol. 17, 1183–1195.
Zoback, M.L., 1992. First- and second-order patterns of stress in the lithosphere: the World Stress Map project. J. Geophys. Res. 97, 11,703–11,728.